PONTIFICAL CATHOLIC UNIVERSITY OF MINAS GERAIS
Chemical Engineering Undergraduate Program

Victor Rezende Moreira
Yuri Abner Rocha Lebron

BIOSORPTION STUDIES: The use of C*hlorella pyrenoidosa* to remediate copper ions and methylene blue from aqueous solutions

Belo Horizonte
2018

Victor Rezende Moreira

Yuri Abner Rocha Lebron

BIOSORPTION STUDIES: The use of C*hlorella pyrenoidosa* to remediate copper ions and methylene blue from aqueous solutions

Undergraduate thesis presented to the Chemical Engineering Undergraduate Program of the Pontifical Catholic University of Minas Gerais (PUC Minas), as a partial requirement to obtain a Bachelor's degree in Chemical Engineering.

Supervisor: Prof.ª Dr.ª Lucilaine Valéria de Souza Santos

Belo Horizonte

2018

Victor Rezende Moreira

Yuri Abner Rocha Lebron

UNDERGRADUATE THESIS

BIOSORPTION STUDIES: The use of C*hlorella pyrenoidosa* to remediate copper ions and methylene blue from aqueous solutions.

Undergraduate thesis presented to the Chemical Engineering Undergraduate Program of the Pontifical Catholic University of Minas Gerais (PUC Minas), as a partial requirement to obtain a Bachelor's degree in Chemical Engineering.

Profª Drª Lucilaine Valéria de Souza Santos.
Supervisor – PUC Minas

Profª Drª Raquel Sampaio Jacob.
Referee – PUC Minas

Prof. Dr. Bruno Rocha Santos Lemos.
Referee – PUC Minas

Drª Fernanda Palladino Pedroso.
Referee – UFMG

Belo Horizonte, 08/11/2018

“Chemical Engineers are not gentle people, they like high temperatures and high pressures”

Steve LeBlanc

“*Success is measured not so much by the position once has reached in life, as by the obstacles one has overcome while trying to succeed*.”

Brooker T. Washington

ACKNOWLEDGMENTS

We thank God for the gift of life, for our health and for always blessing us, our family and our friends.

From Yuri:

I would like to express my infinite gratitude for my parents Luciana Rocha and Jorge Ferreira for all dedication, love, affection, understanding, motivation, zeal and advices. You are my greatest examples of character and determination, are my sources of inspiration for me to continue to pursue my goals. Thank you so much for always supporting me.

I thank the friends I made at PUC-Minas and UFMG-DESA during these years, especially my partner Victor Moreira. Thank you so much for every word of motivation. Thank you for believing in my work and spending so many moments, goods and bads, by my side. I thank God for putting you in my life, I believe that this partnership and trust that I have deposited in you would not work with anyone else. I would not have achieved the things I achieved without your strength, tranquility, advice and companionship, thank you!

From Victor:

They say that the first step to show gratitude is to remember the reasons for being grateful. In this way, I would like to express my thanks to those people who have allowed me to go through singular moments over these years. To my parents, João Célio and Maria José, who encouraged me and gave me the opportunity to achieve this victory. My sister, Larissa, for the example of determination and perseverance. To all of you, who in the moments of my absence have always made me understand that the future is made from constant dedication in the present, my eternal thank you! To the masters and teachers who have been present throughout these years. I am also grateful to all of my friends and colleagues who have been part of my academic training and will certainly continue to be present in my life. Of all these, I could not fail to mention the great friend and companion of these last years, Yuri Lebron. To you my immense gratitude for all the moments and conquests of which I recognize that they would not be possible if I were not part of them. I am extremely grateful to all those who contributed directly or indirectly and acknowledge that this is only the first step towards a future that is still uncertain and little known. In any case, I do not fear the future, for He who guided me here will guide me to the end.

We would like to express my gratitude to all teachers of the chemical engineering department of PUC-Minas, especially our supervisor Lucilaine Valéria, for all teaching, conversations, advice and patience. You, who possesses the gift of teaching with simplicity, knew how to arouse admiration and became inspiration. Thank you so much for having trusted in our work thus contributing to our personal and professional growth.

We would like to thank the lab technician Thais Munique for always helping us and clarifying any doubts.

Finally, we would like to thank the teachers Fernanda Palladino, Bruno Rocha and Raquel Sampaio for kindly accepted the invitation to participate as referees.

ABSTRACT

The discharge of effluents contaminated with heavy metal ions and dyes represents a serious environmental problem. Currently the processes employed have some drawbacks, hence, the biosorption process by microalgae has attracted attention, but studies related to copper and methylene blue (MB) biosorption by *Chlorella pyrenoidosa* are scarce. The present work aimed to characterize, verify thermodynamic viability and optimize the MB and copper biosorption onto *Chlorella pyrenoidosa* using a Box-Behnken factorial design. The adsorbent had a particle diameter ranging from 14.13 to 123.6 μm, with macropores of 1.868 ± 0.337 μm. The infrared spectrum of the adsorbent indicated a physical adsorption mechanism that was later proven by the enthalpy change. The biosorption was shown to be thermodynamically feasible since the values of Gibbs free energy change were negative. The quadratic model obtained by the Box-Behnken factorial design showed high correlation coefficient and low residuals, being adequate for the prediction of the response variable. The maximum removal efficiency obtained by optimization was 83.14% when the algae concentration was 1.28 $g.L^{-1}$, 5 $mg.L^{-1}$ of copper and pH 6.33. Regarding MB biosorption the maximum value obtained was 98.20% when the algae concentration was 0.29 $g.L^{-1}$, 10.67 $mg.L^{-1}$ of MB and pH 6.62.

Keywords: *Chlorella pyrenoidosa*. Biosorption. Copper. Methylene Blue. Optimization.

FIGURES LIST

TABLES LIST

ABBREVIATIONS LIST

$2FI$	Two-factor interaction model
$\Delta G°$	Gibbs free energy change (kJ.mol^{-1})
$\Delta H°$	Enthalpy change (kJ.mol^{-1})
$\Delta S°$	Entropy change (kJ.K^{-1}.mol^{-1})
χ^2	Chi-square
$\%Removal$	Removal efficiency (%)
A	Coded factor – Copper concentration (mg.L^{-1})
$ANOVA$	Analysis of variance
A_t	Temkin equilibrium binding constant (L.g^{-1})
B	Coded factor – pH
b	Temkin isotherm constant related to the adsorption heat (J.mol^{-1})
BBD	Box-Behnken design
C	Coded factor - Biosorbent concentration (g.L^{-1})
C_e	Equilibrium concentration (mg.L^{-1})
C_f	Final concentration (mg.L^{-1})
$CFEF$	Composite fractional error function
C_i	Initial concentration (mg.L^{-1})
$C_{M^{n+}}$	Cations concentration (mg.L^{-1})
$C.pyrenoidosa$	*Chlorella pyrenoidosa*
$C.V.\%$	Coefficient of variation (%)
D	Coded factor – Methylene blue concentration (mg.L^{-1})
df	Degrees of freedom
E	Average energy of adsorption (kJ.mol^{-1})
EDS	Energy dispersive X-ray spectroscopy
$FTIR$	Fourier Transform Infrared Radiation
h_0	Initial adsorption rate (mg.g^{-1}.min^{-1})
k_1	Pseudo first order rate constant (min^{-1})
k_2	Pseudo second order rate constant (g.mg^{-1}.min^{-1})
K_d	Distribution coefficient
K_{DR}	Dubinin-Radushkevich equilibrium constant
k_f	Freundlich equilibrium constant (mg$^{1-1/n}$.L$^{1/n}$.g^{-1})
k_l	Langmuir equilibrium constant (L.mg^{-1})

L	Linear model
$L-M$	Levenberg-Marquardt
m	Mass of the biosorbent (mg)
MB	Methylene Blue
N	Number of experimental samples
n	Freundlich equilibrium constant
pH_{PZC}	Point of zero charge
$PRESS$	Predicted residual sum of squares
Q	Quadratic and cubic models
q_e	Biosorption capacity ($mg.g^{-1}$)
$q_{e,calc}$	Theoretical value of biosorption at equilibrium ($mg.g^{-1}$)
$q_{e,exp}$	Experimental value of biosorption at equilibrium ($mg.g^{-1}$)
$q_{e,i}$	Biosorption capacity corresponding to cycle i ($mg.g^{-1}$)
$q_{e,max}$	Maximum experimental biosorption capacity ($mg.g^{-1}$)
q_m	Maximum theoretical value for the adsorption capacity ($mg.g^{-1}$)
q_s	Dubinin-Radushkevich theoretical isotherm saturation capacity ($mg.g^{-1}$)
q_t	Biosorption capacity at a given time ($mg.g^{-1}$)
R	Ideal gas constant ($8.314\ J^{-1}.K^{-1}.mol^{-1}$)
R^2	Correlation coefficient
Re	Regeneration efficiency (%)
$R_{b/r}$	Ion exchange ratio
R_L	Separation factor
SEM	Scanning electron microscopy
SS	Sum of squares
SSE	Sum of error square
$Std.Dev.$	Standard deviation
$t_{0.5}$	Half adsorption time or half-life (min)
T	Absolute temperature (K)
t	Time (min)
TGA	Thermogravimetric analysis
v	Total volume of medium (L)
y_{calc}	Calculated data
y_{exp}	Experimental data

SUMMARY

1. INTRODUCTION

Effluents contaminated with heavy metal ions and dyes represent a serious environmental problem which has been raising global attention due to the potential of imposing threats to human health and wild life. Heavy metal ions reach water source mainly from electroplating, mining, metal processing, and metallurgy industries wastewater. In addition to environmental damage, they also affect living beings, as metals have a potential to bioaccumulate (DINU; DRAGAN, 2010). Copper was one of the first heavy metals used by mankind, in addition to be a very abundant metal. Although classified as heavy metal, copper is essential to human health, and its daily intake varies between 0.9 and 2.2 mg for adults (MOURA, 2001). However, the presence of this element is toxic at concentrations above 1.3 $mg.L^{-1}$ (EPA, 2005) and it is associated with changes in the nervous system, gastrointestinal irritation, depression and lung cancer (MANZOOR et al., 2013).

As for dyes and pigments, they are widely used in the textile, food, paper and cosmetics industries. Among the manufacturing sectors, the textile industry is one of the most significant in water consumption in its processes - between 60 and 100 kg per kilogram of fabric dyed and washed (COUTO; MORAVIA; AMARAL, 2017), and for this reason a significant amount of effluent is generated in this segment. Without proper treatment, the discharge of these effluents is associated with several environmental problems and has been a major concern over the years. Even so, these compounds are considered recalcitrant and difficult to remove, since they are stable to light, heat and oxidizing agents (GUPTA; SALEH, 2013).

Several processes have been developed in order to reduce the presence of dyes and heavy metal ions in water sources. Among those are the reverse osmosis processes, oxidative processes, activated carbon adsorption, ion exchange and coagulation, all of which exhibits a considerable removal efficiency, but also some disadvantages. Biological treatments may have low effectiveness as a result of the low biodegradability of dyes, especially at low concentrations, in addition to a toxic sludge generation (FOROUGHI-DAHR et al., 2015b). For the oxidative processes, some organic compounds may be formed such as 2-aminophenol, 2-amino-5-(methylamino)-hydroxybenzenesulfonic acid and 2-amino-5-(N-methylformamido)-benzenesulfonic acid, all identified by Xia et al. (2015) when evaluating the photocatalytic degradation process of methylene blue. The formation of by-products leads to the necessity of further treatment after the oxidation step impacting on higher operational costs (YAGUB et al., 2014).

A study developed by Xu et al. (2018) emphasized the biosorption advantages compared to other techniques used to remove heavy metals from aqueous media. Among them are high removal capacity, low cost, ease of operation and applicability over a wide pH range. Although the technique is considered to present a low selectivity, it still stands out against membrane separation processes, ion exchange and electrochemical removal, considered of high cost and difficult regeneration. Romero-Cano et al. (2017) highlighted that although activated carbon is the most used adsorbent material, its cost is still high. For that reason, several studies have been carried out aiming the search for natural adsorbents (SOLISIO; AL ARNI; CONVERTI, 2017), due to the great variety of biological materials available and their ability to promote metals and dyes retention.

In general, an adsorbent can be classified as low cost if it requires little processing in its obtainment, is abundant in nature or considered as waste material/by-product of industrial activities (YAGUB; SEN; ANG, 2014). Recently, considerable efforts have been devoted in order to develop natural and low-cost adsorbent such as tea waste (FOROUGHI-DAHR et al., 2015a), corn stalk (CHEN et al., 2012), *Cucumis sativus* peel (LEE et al., 2016), white pine (SALAZAR-RABAGO et al., 2017), chestnust husk (GEORGIN et al., 2018), among others. Biological materials, namely biosorbents, are also considered low cost and have advantages like greater selectivity when compared to ion exchange and activated carbons. An example of biosorbent are the algae, showing a promise application in the biosorption process.

Microalgae are unicellular species, commonly found in marine and freshwater with the size ranging from a few micrometers to a few hundreds of micrometers. It has been estimated that 2×10^5 to 8×10^5 species exist. The three most important classes of microalgae in terms of abundance are the diatoms (*Bacillariophyceae*), the green algae (*Chlorella*), and the golden algae (*Chrysophyceae*) (PIRES, 2015). *Chlorella*, one of the prime targets of the algae industry, is a unicellular green alga found in both fresh and marine water. Its popularity in the Far East has been based on the belief, and more recently, on scientific evidence that it can have health benefits (SUÁREZ et al., 2005). They present several advantages over other adsorbents such as their large availability in several regions of the world and the possibility to be cultivated in freshwater and saltwater under various climatic conditions, resulting in a low cost in their preparation (PIRES, 2015).

In view of these considerations the present work aimed to evaluate the copper and methylene blue (MB) biosorption process using dried biomass of *C. pyrenoidosa* algae as a biosorbent.

2. OBJECTIVES

2.1 General

The present work aimed to evaluate the copper and methylene blue (MB) biosorption process using dried biomass of *Chlorella pyrenoidosa* algae as a biosorbent.

2.2 Specifics

i. Characterize the *Chlorella pyrenoidosa* used in this work;
ii. Evaluate kinetics parameters;
iii. Verify the equilibrium using isotherms models;
iv. Evaluate thermodynamic parameters;
v. Optimize the parameters involved for maximum copper and MB removal efficiency.

3. LITERATURE REVIEW

3.1 Heavy metals and sources of contamination

In recent years, awareness of the need for the rational use of natural resources and the development of technologies that minimize environmental impacts is more evident as a result of the growing concern of the world's population with environmental damage. Among the environmental components, water bodies are most affected by pollution in Brazil, as a consequence of their effective participation in the economic and biological processes that structure society (GÓMEZ, 2014; PINO, 2005; RAULINO, 2016).

Metals are present in naturally occurring biogeochemical cycles. However, notably there is a significant increase in the concentration of some of them, mainly due to the growth of industrial activities (SILVA, 2017). Heavy metals constitute a group of approximately 40 elements, having its elementary form with a density equal to or greater than 5 $g.cm^{-3}$ or when its atomic number is greater than 20. Currently its presence in the earth's crust is less than 0.1% (VILLANUEVA, 2000). Examples of heavy metals are: Cadmium (Cd), Chrome (Cr), Copper (Cu), Mercury (Hg), Nickel (Ni), Lead (Pb) and Zinc (Zn), whose presence is usually associated with problems related to pollution and toxicity (RAULINO, 2016; SILVA, 2017).

The main sources of heavy metals are industrial waste from processes such as electroplating, mining, nuclear fuel processing, photography, batteries, production and recovery of catalysts, paints, automotive industry and other extraction, production, treatment, cleaning or finishing procedures of metals (SCHULTZ, 2003). For several decades, the national production of Pb, Zn, Fe and Cu were estimated at 200,000 tons per year (SOUZA et al., 2016). Besides the metallurgical industry, domestic solid waste accounts for a large part of the contribution (50-80%) in the presence of Zn, Pb and also Cu in the environment (BOLLER, 1997).

Although classified as heavy metal, copper is a metal essential to human health, being present in all fluids and many human tissues and the daily intake of this metal varies between 0.9 and 2.2 mg for adults (MOURA, 2001). This element, along with amino acids, fatty acids and vitamins, is required for metabolic processes. However, the presence of this element is toxic at concentrations above 1.3 $mg.L^{-1}$ (EPA, 2005), due to the affinity of the metal with SH groups of many proteins and enzymes, being associated with diseases such as epilepsy, melanoma and arthritis rheumatoid arthritis, as well as loss of taste. Brazil through the National Environmental Council published in 2011 n° 430 that deals with maximum acceptable values for the release of industrial effluents in receiving bodies, and for the copper in question this limit is 1 $mg.L^{-1}$.

Souza et al. (2016) evaluated the heavy metals Cd, Cr, Cu, Fe, Mn, Ni, Pb and Zn present in surface water from two regions of the lower São Francisco River, the first located in the city of Petrolina-PE and the second one in Juazeiro- BA. Both cities, together, can be classified as metropolis and present several industrial segments and possible sources of contamination of heavy metals. Among the heavy metals detected, copper was present in all samples evaluated at concentrations that reached 0.596 $mg.L^{-1}$.

3.2 Dyes and sources of contamination

Dyes are pollutants that are difficult to remove from effluents because they are generally not biodegradable and are toxic to plants, animals and humans (KHATAEE; VAFAEI; JANNATKHAH, 2013). The greatest environmental impact caused by dyes is the reduction of the absorption of the sunlight that enters the water, which interferes in the growth of bacteria, interfering in the biological degradation of water impurities (BONILLA-PETRICIOLET; MENDOZA CASTILLO; REYNEL-ÁVILA, 2017). In addition, algae growth slows down as sunlight does not reach them; some algae die, affecting the food chain. The dye molecules are distinguished by their large size, which is why adsorbents with a larger pore size are preferable (GEORGIN et al., 2018).

These compounds are widely used in various industrial segments such as plastics, leather tanning and especially in the textile industries (LEE et al., 2016). In the latter, for example, it is estimated that between 60 and 100 kg of water are used for each gram of dyed and washed fabric (COUTO et al., 2017), and for this reason a large amount of effluent is generated in this segment.

Dyes can be classified according to their structure, application, color and also their charge depending on the medium in which it is encountered (SALLEH et al., 2011; YAGUB et al., 2014). Thus, they are subdivided into anionic (direct, acid and reactive dyes; i.e. Reactive Black 5 and Acid Blue 71), non-anionic (dispersed dyes; i.e. Dispersed Orange 5) and cationic (all basic dyes; i.e. Methylene Blue) (SALLEH et al., 2011).

Among the cationic dyes, methylene blue (MB), $C_{16}H_{18}N_3SCl$, stands out due to its applicability in several industrial segments such as hair coloring; paper and silk dyeing; cotton and its use as a standard for testing adsorbents (KAZEMI et al., 2013; MIRABOUTALEBI et al., 2017; PEYDAYESH; RAHBAR-KELISHAMI, 2015). Consumption at high concentrations of MB is associated with respiratory distress, nausea and mental disorder, and its toxicity is attributed to the presence of amine groups that constitute it (MITROGIANNIS et al., 2015). For

these reasons, the compound is considered in several studies that aim to evaluate the removal of cationic dyes from contaminated effluents.

3.3 Remediation techniques currently employed

Treatment of effluents containing heavy metal ions or dyes is still a major economic challenge. Among the currently used processes are the chemical precipitation (CHARERNTANYARAK, 1999), ion exchange (DĄBROWSKI et al., 2004), membrane separation processes (QDAIS; MOUSSA, 2004) and adsorption (LEE; LALDAWNGLIANA; TIWARI, 2012). However, the high cost associated with the chemical reagents used when these processes are considered in industrial scale, besides the low percentage of removal in some of these processes, make them unfeasible (ZERAATKAR et al., 2016).

Specifically, the processes involving precipitation are considered in many cases unfavorable, especially for the case when heavy metals are present at low concentrations. Moreover, these processes are accompanied by flocculation and coagulation stages, responsible for the formation of large quantities of sediment with high concentration of these pollutants (DHIR, 2014). Among the membrane separation processes the most used are reverse osmosis (RO) and nanofiltration (NF), which were initially developed for the purification of salt water (QDAIS; MOUSSA, 2004). However, these processes have been considered in other applications such as the treatment of industrial effluents. Although they present good percentage of removal of these contaminants, they have the disadvantage of the generation of toxic and concentrated sludge (GAUTAM et al., 2014).

For the treatment of dyes, either cationic or anionic, some technologies such as oxidation and ozonation have still been considered as a result of their good removal efficiency, even though they present high installation and operational costs. An alternative to these processes is the biological anaerobic treatments which, despite the high rate of degradation for some dyes, complete mineralization of others is difficult to be obtained and results in compounds such as aromatic amines that present a toxic and carcinogenic character (O'MAHONY; GUIBAL; TOBIN, 2002).

Based on these reasons, associated to more restricted standards for effluents discharge and more stringent water potability standards, more efficient techniques that present lower costs are necessary.

3.4 Adsorption

Adsorption has become one of the most popular methods to remediate water contamination, gaining importance as a process of separation and purification in the last decades. The process has several advantages over conventional treatment methods such as regeneration capability, reuse of material, effectiveness at trace concentrations and low cost in nature (DEMIRBAS, 2008). It has been an object of interest to scientists since the beginning of the century, presenting technological and biological importance, as well as practical applications in industry and environmental protection, making it a useful tool in several sectors. Currently, the adsorption is one of the most efficient water and wastewater treatment processes employed in industries to reduce their effluent levels (NASCIMENTO et al., 2014).

Adsorption is a mass transfer operation where molecules of a fluid phase called adsorbate meet spontaneously on a generally solid surface defined as adsorbent, allowing the separation of the components of these fluids (NASCIMENTO et al., 2014). This is a fundamental property of matter, having its origin in the attractive forces between molecules (MOURA, 2001). According to the nature of the forces involved the adsorption process can be classified as: physical adsorption and chemical adsorption.

In a physical adsorption process, the attractive effects that occur between the adsorbent and adsorbate are considered relatively weak, involving mainly Van der Waals interactions. This process is reversible, not specific and usually occurs with the deposition of more than one layer of adsorbate over the adsorbent (SILVA, 2010). As a consequence, the adsorption force decreases as the number of layers increases (NASCIMENTO et al., 2014).

Differently from the physical adsorption, the chemical adsorption results from a more intense interaction between the adsorbed substance and the adsorbent. For this type of adsorption, there is a significant number of electrons being transferred, equivalent to the formation of a chemical bond between the adsorbate and the solid surface. Such interactions are stronger and more specific than physical adsorption forces and for most cases are limited to monolayer cover (SILVA, 2010).

Regardless of the nature of the interactions between adsorbate and adsorbent, the adsorption process can be altered by several factors, for example, type of adsorbent and adsorbate, physico-chemical characteristics and operational conditions. An increase in temperature of the system causes, in most cases, a decrease of the amount adsorbed by the solid, if the processes present an exothermic heat of adsorption. In other few cases an opposite behavior is observed, in which the temperature increase favors the adsorption process, being

these processes classified as endothermic. The size of the particle, the amount of adsorbate and the amount of adsorbent in the system also change the process. Since the adsorbed components concentrate on the outer surface, the larger the outer surface per unit of solid mass, more favorable the adsorption will be. Therefore, adsorbents are generally solids with porous particles (NASCIMENTO et al., 2014). Operational conditions such as pH of the medium can cause significant modifications in the adsorption of the component of interest (SILVA, 2010).

In summary, the adsorption separation processes are based on three distinct mechanisms: the steric mechanism, the equilibrium mechanisms and the kinetic mechanisms. For the steric mechanism, the pores of the adsorbent material have characteristic dimensions, which allow certain molecules to enter, excluding the rest. The equilibrium mechanisms are related to the abilities of the different solids to accommodate different species of adsorbates. Finally, the kinetic mechanism is based on the different diffusivities of the various species in the adsorbent pores (BONILLA-PETRICIOLET; MENDOZA CASTILLO; REYNEL-ÁVILA, 2017).

3.4.1 Equilibrium isotherms

The adsorption equilibrium is generally an essential requirement for obtaining relevant information on the design and analysis of an adsorption separation process. When a certain amount of an adsorbent comes in contact with a given volume of a liquid containing an adsorbate the adsorption occurs until the equilibrium is reached. That is, when the adsorbate is contacted with the adsorbent, the molecules or ions tend to flow from the aqueous medium to the surface of the adsorbent until the solute concentration in the liquid phase remains constant. At this stage it is said that the system reached equilibrium and the adsorption capacity of the adsorbent is determined (BONILLA-PETRICIOLET; MENDOZA CASTILLO; REYNEL-ÁVILA, 2017; VIDAL et al., 2016). There are several types of isotherms, with several proposed mechanisms and equations. Among the most used isotherms models are: Langmuir, Freundlich, Dubinin-Radushkevich and Temkin.

The Langmuir model calculates the amount of molecules adsorbed onto a solid surface and is often used to describe the solute adsorption (LANGMUIR, 1918). This model assumes a monolayer adsorption onto a complete homogeneous surface with a negligible interaction between adjacent adsorbed molecules. The Langmuir model equation is one of the most used equations for the representation of adsorption processes (BONILLA-PETRICIOLET; MENDOZA CASTILLO; REYNEL-ÁVILA, 2017; NASCIMENTO et al., 2014).

The Freundlich equation is an empirical equation proposed by Freundlich. It is commonly used to describe the adsorption of organic components in solution; it assumes that the adsorption sites are not identical. It usually applies to heterogenous surfaces and multilayer adsorption on the adsorbate is considered in this model (NASCIMENTO et al., 2014; PINO, 2005). Both Langmuir and Freundlich isotherm models are simple, give a good description of experimental behavior in a large range of operating conditions and are recharacterized by a limited number of adjustable parameters (AKSU; DÖNMEZ, 2006).

The Temkin model is a two-parameter equation that takes into account adsorbent-adsorbate interactions and the uniform distribution of binding energies (FOO; HAMEED, 2010). Disregarding extremely low or extremely high concentrations, the model assumes that the adsorption heat of the molecules in the layer tends to decrease linearly - not logarithmically - with the increasing coverage degree of the adsorbent. His equation was initially proposed to describe the adsorption of hydrogen on platinum electrodes in acid medium (AHARONI; UNGARISH, 1977). Temkin isotherm model is most commonly used for gaseous systems (KIM et al., 2004), since many factors that participate in the complexity of liquid systems are not considered in the development of the model, for example, pH, the organization of molecules on the surface of the adsorbent and even the solubility of the solute in the liquid medium in question (NASCIMENTO et al., 2014).

The Dubinin-Radushkevich equation describes quite satisfactory equilibria of adsorption of organic compounds in gas phase on solid adsorbents. Similarly to the Temkin equation, the Dubinin-Radushkevich equation does not consider aspects that make up the equilibrium complexity in liquid medium, such as pH, ionic equilibria and solute-solvent interactions (FEBRIANTO et al., 2009).

3.4.2 Kinetic models

Adsorption kinetics is expressed as the rate of removal of adsorbate in the fluid phase with respect to time. It involves the mass transfer of one or more components contained in an external liquid mass into the adsorbent particle, which shall migrate through the pores to the innermost regions of this particle (NASCIMENTO et al., 2014). There is a variety of models widely utilized to describe the kinetic adsorption process, differing itself by the assumptions made. In principle, adsorption kinetics can be driven by three different processes: external mass transfer from bulk-solution, diffusion in the pore and surface diffusion, all represented in Figure 1.

Figure 1 - Adsorption mechanism diagram.

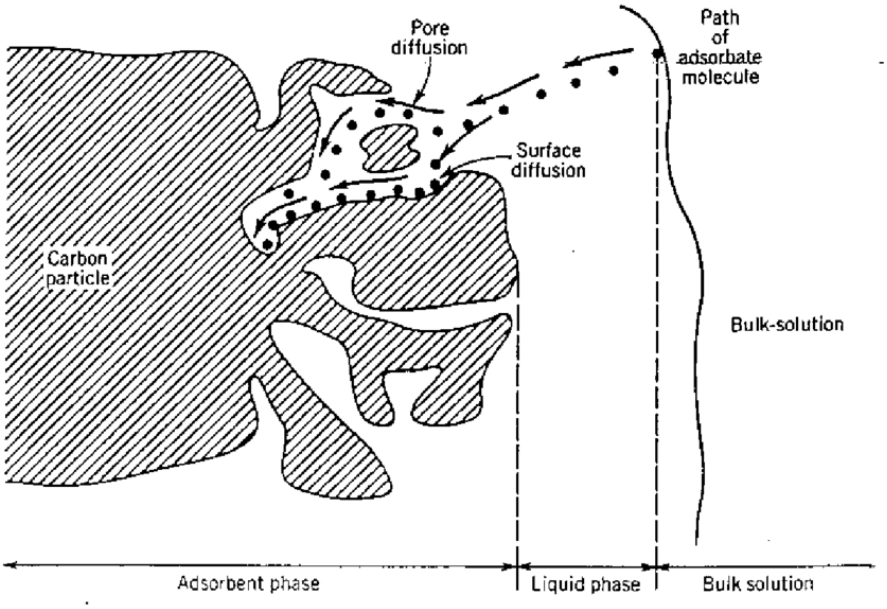

Source: MOURAD et al., 2012

External mass transfer corresponds to the ions or molecules transfer from the fluid phase to the outer surface of the adsorbent particle, by means of a layer of fluid surrounding the particle. The second one, diffusion in the pore, is caused by the diffusion of species from the fluid into the pores. Finally, the surface diffusion process corresponds to the diffusion of fully adsorbed molecules along the surface of the pore (NASCIMENTO et al., 2014).

In general, adsorption velocity can be affected by temperature, pH, ionic strength, initial adsorbate concentration, agitation, particle size and pore size distribution(MCKAY, 2007). Among these, the first stage is significantly affected by adsorbate concentration and agitation (CHEUNG; SZETO; MCKAY, 2007). Therefore, an increase in the concentration of the solute may accelerate its diffusion to the surface of the solid. The second step is generally considered the determining step, especially in the case of microporous adsorbents (CHEUNG; SZETO; MCKAY, 2007).

In batch systems, the most applied models are the pseudo-first-order and pseudo second-order (LARGITTE; PASQUIER, 2016; QIU et al., 2009). These models are originally non-linear, even though their linear forms are widely used in several studies (SOLISIO; AL ARNI; CONVERTI, 2017; VAZ et al., 2017; WONG et al., 2018). Regardless, these models are used in order to evaluate the controlling mechanism of the adsorption process, such as chemical reaction, diffusion control and mass transfer.

3.4.3 Adsorption thermodynamics

The flow of energy between the system and the neighborhood can be used as a criteria of spontaneity. Those in which the energy leaves the system are denominated exergonic ($\Delta G<0$) and, therefore, spontaneous. Conversely, when the energy brings into the system ($\Delta G>0$), the process is said to be endergonic, and is not spontaneous (NASCIMENTO et al., 2014; PETER ATKINS, 2006).

These observations also apply to the phenomenon of adsorption, which is physicochemical in nature. In adsorption, attractive forces act in order to allow the covering of a given surface, by related species, so that there is always release of free energy. Thus, whenever at a given temperature the Gibbs energy variation relative to the adsorption process is negative ($\Delta G<0$), the process will occur spontaneously, although nothing can be predicted about the time required for it to occur (BONILLA-PETRICIOLET; MENDOZA CASTILLO; REYNEL-ÁVILA, 2017; NASCIMENTO et al., 2014; PETER ATKINS, 2006).

The estimation of the values for the thermodynamic parameters of the adsorption is of great utility and importance. Among other things, it allows:

• Determine if the process is feasible, that is, spontaneous;

• Whether it is governed mainly by enthalpic or entropic contributions;

• Indicate the nature of the process (physical or chemisorption).

For this last point, kinetic aspects need to be considered (NASCIMENTO et al., 2014).

The most widely used thermodynamic parameters in these studies are equilibrium constant (K_d), Gibbs energy variation (ΔG^o), enthalpy change (ΔH^o) and entropy variation (ΔS^o).

3.4.4 Biosorbents

The biosorption process has been shown to be a promising technology in the treatment of effluents and surface waters. In general, the process uses by-products such as lignocellulosic material, even though microorganisms has been widely used in past years due to the facilities associated with its cultivation (JAIN; MALIK; YADAV, 2016). Among the biomass byproducts the following stand out due to their biosorption capacity: seeds, leaf, husk and bark, as they usually presents several functional groups in their constitution (DHIR, 2014), resulting in a high removal efficiency of certain species.

These materials can be considered low cost since they are widely found in a natural way, some still freely available as they are designated as waste in the processing of lignocellulosic

materials and require little or no previous processes prior to its use as adsorbent. Algae, in general, stand out among these materials once they are available in large quantities, in several regions of the world, are easy to grow, even in salt water or wastewater (PIRES, 2015).

The biosorption process by algae is due to two main mechanisms, a passive uptake process or through its metabolic activity when used in its living form. However, the use of dry biomass of algae has stood out against live microorganisms because of the following advantages. The dry biomass can be easily stored for long periods of time without refrigeration, there is no loss of its properties and characteristics as biosorbent while stored, they are not affected by the potentially toxic character of the species to be treated and may have a superior adsorption capacity if compared to the same algae alive, already proved by some studies (GAUTAM et al., 2014; PIRES, 2015). This process already has many advantages that can still be optimized through a powerful statistical tool, surface response methodology (RSM).

3.5 Microalgae

There are more than 50,000 species of microalgae, they are a very diverse group of unicellular, predominantly aquatic and photosynthetic organisms that account for almost 50 % of the photosynthesis that takes place on Earth. Algae have a wide range of antenna pigments to harvest light energy for photosynthesis giving different types of algae their characteristic color (BLINOVÁ; BARTOŠOVÁ; GERULOVÁ, 2015). Algae are proposed to play a role in the global carbon cycle by helping remove excess carbon dioxide from the environment. Depending on size, algae are classified as microalgae or macroalgae (seaweed). Microalgae are categorized as prokaryotes and eukaryotes being the organelles are the major difference between them. Prokaryotes do not possess chloroplast, mitochondria and nuclei but they contain chlorophyll a and high protein contents. Microalgae are further divided into different groups based on their taxonomy, including blue-green, green, yellow-green, red, brown, and golden algae (MORONEY; YNALVEZ, 2009; RASHID et al., 2014).

Microalgae can also be categorized based upon carbon supply. Some microalgae use inorganic carbon such as CO_2, are known as autotrophs. Autotrophs perform photosynthesis using light as energy source while heterotrophic microalgae use organic carbon as sugars. There are some species which can use both, organic and inorganic carbon sources, are called mixotrophs (RASHID et al., 2014; DAHIYA, 2014).

3.5.1 Chlorella pyrenoidosa

Chlorella, one of the prime targets of the algae industry, is a unicellular green alga found in both fresh and marine water. Its popularity in the Far East has been based on the belief, and more recently, on scientific evidence that it can have health benefits (SUÁREZ et al., 2005). They present several advantages over other adsorbents such as their large availability in several regions of the world and the possibility to be cultivated in freshwater and saltwater under various climatic conditions, resulting in a low cost in their preparation (PIRES, 2015).

3.6 Response Surface Methodology

Usually one of the most commonly encountered problems in performing experiments is in determining the influence of one or more variables on the system under study. To plan any experiment, the first step is to decide what are the interfering factors and the influence of the variables controlled by the experimenter, as well as the responses of interest. The factors can be qualitative or quantitative. It is also necessary to define the objective of the experiment to choose the most appropriate type of planning (CALADO; MONTGOMERY, 2003). Factorial planning is a statistical tool that determines whether the factors chosen to be studied in a system has or does not influence the response of this system. It also allows to evaluate the level of this influence and the existence of interaction between the variables (CALADO; MONTGOMERY, 2003; RODRIGUES FILHO, 2012).

Response surface methodology (RSM) is a collection of mathematical and statistical techniques for empirical model building. By careful design of experiments, the objective is to optimize a response (output variable) which is influenced by several independent variables (input variables). An experiment is a series of tests, called runs, in which changes are made in the input variables in order to identify the reasons for changes in the output response (CALADO; MONTGOMERY, 2003).

Originally, RSM was developed to model experimental responses (BROWN; BOX; DRAPER, 1990), and then migrated into the modelling of numerical experiments. The difference is in the type of error generated by the response. In physical experiments, inaccuracy can be due, for example, to measurement errors while, in computer experiments, numerical noise is a result of incomplete convergence of iterative processes, round-off errors or the discrete representation of continuous physical phenomena. In RSM, the errors are assumed to be random (GIUNTA; WATSON, 1998; TOROPOV et al., 1996; VAN CAMPEN, D.H., NAGTEGAAL; A.J.G., 1990).

4. MATERIALS AND METHODS

4.1 Reagents and chemicals

Biosorption experiments were performed using dried biomass of *C. pyrenoidosa* algae acquired at the farm "A Floresta - Ervas medicinais", Esmeraldas - MG (19°42'08.0"S, 44°11'43.3"W). The samples were stored in the absence of light and humidity and all the reagents used were of analytical grade. Ultrapure water (ThermoScientific Smart2Pure 3 UV) was used to prepare all solutions. Working solutions of copper and MB (3000 $mg.L^{-1}$) were prepared from hydrated copper sulfate - $CuSO_4.5H_2O$ (Synth) and MB (Exôdo Cientifica®), respectively. The pH of the solutions was adjusted using hydrochloric acid or sodium hydroxide both 0.1 $mol.L^{-1}$ (Synth). For the preparation of calibration curves a standard copper solution of 1000 $mg.L^{-1}$ (SpecSol) was used.

4.2 Instrumentation

Copper concentration analysis were performed in a flame atomic absorption spectrometer (Shimadzu, AA-7000) equipped with deuterium lamp to make background correction. A hollow cathode lamp at 324.8 nm was used to measure the concentrations of Cu (II), the lamp current was 8 mA, burner high of 7.0 mm and a slit width of 0.7 nm. An air/acetylene flame with flow rates of 15.0 and 1.8 $L.min^{-1}$, respectively, was used. The calibration range was between 0.5-10 $mg.L^{-1}$ (R^2>0.99). The instrument was operated under conditions recommended by the manufacturer.

MB concentrations were determined by a UV-Vis (Shimadzu UV 3600) spectrophotometer with the aid of a calibration curve ranging from 0.5 to 15 $mg.L^{-1}$ (R^2>0.99) in the wavelength of 665 nm. The wavelength considered corresponded to the maximum absorbance wavelength observed after a spectrum scan of the MB working solution.

pH was measured using pHmeter (HANNA, HI2020) calibrated using two buffers (4 and 7).

4.3 *Chlorella pyrenoidosa* characterization

C. pyrenoidosa sample was characterized in terms of its composition and morphology. FTIR analysis (Shimadzu IRAffinity-1) was conducted in the region of 750-4000 cm^{-1} with resolution of 4 scans per second and a total of 20 scans. The biosorbent was analyzed before and after the biosorption process, both at the same background and using ATR as the sample

technique. Thermogravimetric analysis was performed at the temperature range of 25 – 800 °C, in alumina (Al_2O_3) crucible with N_2 flow of 50 mL.min^{-1}, to avoid oxide formation, and a heating rate of 10 °C.min^{-1} (Shimadzu DTG-60H).

The point of zero charge (pH_{PZC}) was defined by the immersion technique, consisted of preparing a 0.5 g.L^{-1} solution of biosorbent in 0.03 mol.L^{-1} sodium chloride (NaCl) solution, adjusting the pH to different values (4-10). The mixture was placed in a shaker (Marconi MA420) for 48 h at 250 rpm and 28 °C and pH_{PZC} was obtained in the range where the buffer effect was observed (FREITAS; CÂMARA; FREIRE, 2015).

Size, morphology and biosorbent surface composition were observed by scanning electron microscopy (SEM) and energy dispersive X-ray spectroscopy (EDS), (JEOL JSM IT300). All the analysis regarding the biosorbent characterization were performed at the Pontifical Catholic University of Minas Gerais' laboratories.

4.4 Biosorption experiments

4.4.1 Box–Behnken Experiment design

Response surface methodology was used in this study to remove systematic errors, produce an estimate of the experimental error and minimize the number of experiments (OVEISI et al., 2017; SALEH; SARI; TUZEN, 2017). A total of 15 experiments were employed to evaluate the effects of the three independent variables (pollutant concentration, pH and *C. pyrenoidosa* concentration) on either copper removal efficiency or MB removal efficiency, including three center replications to assess the pure error. The Box-Behnken design (BBD) was used to investigate the parameters involved with the levels coded as -1 (lower level), 0 (center point) and +1 (upper level). Table 1 shows a factorial design matrix used to evaluate the copper removal process and

Table 2 a factorial design matrix for the MB removal process. Statistical analysis was carried out in the Statistica software (StatSoft Inc. 2011), version 11.

Table 1 - Factorial design matrix for copper biosorption.

Run order	Coded (real) value		
	A: Copper concentration ($mg.L^{-1}$)	B: pH	C: Biosorbent concentration ($g.L^{-1}$)
1	-1 (5)	-1 (4)	0 (1)
2	1 (15)	-1 (4)	0 (1)
3	-1 (5)	1 (8)	0 (1)
4	1 (15)	1 (8)	0 (1)
5	-1 (5)	0 (6)	-1 (0.5)
6	1 (15)	0 (6)	-1 (0.5)
7	-1 (5)	0 (6)	1 (1.5)
8	1 (15)	0 (6)	1 (1.5)
9	0 (10)	-1 (4)	-1 (0.5)
10	0 (10)	1 (8)	-1 (0.5)
11	0 (10)	-1 (4)	1 (1.5)
12	0 (10)	1 (8)	1 (1.5)
13	0 (10)	0 (6)	0 (1)
14	0 (10)	0 (6)	0 (1)
15	0 (10)	0 (6)	0 (1)

Table 2 - Factorial design matrix for methylene blue biosorption.

Run order	Coded (real) value		
	D: Methylene blue concentration ($mg.L^{-1}$)	B: pH	C: Biosorbent concentration ($g.L^{-1}$).
1	+1 (30)	0 (6)	+1 (0.75)
2	0 (20)	+1 (10)	+1 (0.75)
3	0 (20)	0 (6)	0 (0.5)
4	0 (20)	-1 (2)	+1 (0.75)
5	-1 (10)	0 (6)	-1 (0.25)
6	+1 (30)	+1 (10)	0 (0.5)
7	0 (20)	-1 (2)	-1 (0.25)
8	-1 (10)	-1 (2)	0 (0.5)
9	+1 (30)	-1 (2)	0 (0.5)
10	0 (20)	0 (6)	0 (0.5)
11	0 (20)	0 (6)	0 (0.5)
12	-1 (10)	+1 (10)	0 (0.5)
13	+1 (30)	0 (6)	-1 (0.25)
14	-1 (10)	0 (6)	+1 (0.75)
15	0 (20)	+1 (10)	-1 (0.25)

4.4.2 Batch biosorption studies

The biosorption process was conducted in erlenmeyer's containing 100 mL of medium, prepared according to the experimental design, under constant agitation (250 rpm) and temperature (28 ºC) in an orbital shaker incubator for 24h to ensure equilibrium. For the kinetic assays, media containing 5 $mg.L^{-1}$ of copper ions and 1.5 $g.L^{-1}$ of algae; 100 $mg.L^{-1}$ of MB and 2.25 $g.L^{-1}$ of algae, both at pH 6 were prepared and 1.5 mL aliquots were collected (0; 0.5; 1; 2; 5; 10; 15; 30; 60 and 160 min) and filtered using a 0.45 μm PVDF polar syringe filter (CHROMAFIL® Xtra) for further analysis. The equilibrium involving the copper biosorption process was evaluated from media of different concentrations (7-38 $mg.L^{-1}$), pH 6 and 1.5 $g.L^{-1}$ of biosorbent. In the other hand, equilibrium involving the biosorption of the MB was evaluated from media of concentrations from 1 to 150 $mg.L^{-1}$, pH 6 and 1 $g.L^{-1}$ of biosorbent. As in the other tests, both temperature and agitation were maintained constant until equilibrium was reached.

The biosorption capacity (q_e, $mg.g^{-1}$) was calculated from Equation 1, where C_i ($mg.L^{-1}$) and C_f ($mg.L^{-1}$) are the initial and final concentration in solution, v (L) the total volume of medium and m (mg) the mass of the biosorbent used.

$$q_e = (C_i - C_f).v/m \quad (1)$$

The removal efficiency ($\%Removal$), expressed as percentage, was calculated by Equation 2.

$$\%Removal = 100\,(C_i - C_f)/C_i \quad (2)$$

4.4.3 Desorption and reuse studies

For the regeneration efficiency and reusability study of the *C. pyrenoidosa* biomass, consecutive biosorption-desorption cycles were repeated using the same biomass until a significant reduction of the biosorption capacity was observed. The loaded biosorbent was treated with a solution of HCl (0.5 $mol.L^{-1}$) in a shaker at 250 rpm, 28 °C during 1 h. The biosorption phase consisted of contacting the regenerated biosorbent with a solution containing copper ions or MB under the same regeneration conditions during 2 h (ASFARAM et al., 2018; CHEN et al., 2017). The regeneration efficiency (Re) was obtained through Equation (3).

$$Re\ (\%) = \frac{q_{e,i}}{q_{e,1}} \quad (3)$$

Where $q_{e,1}$ corresponds to the biosorption capacity of the first cycle (mg.g^{-1}), and $q_{e,i}$ to the biosorption capacity of the "i" cycle (mg.g^{-1}).

4.4.4 Ion exchange studies

For these experiments, 0.20 g of *C. pyrenoidosa* was mixed with 100 mL of either copper or MB solution (5 mg.L^{-1}) at pH 6. Two blanks were also carried out; one without the respective adsorbate and the other without *C. pyrenoidosa*. The solutions were stirred at 250 rpm for 2 h at 28 °C. The amount of cations (Ca^{2+}, Mg^{2+}, Na^{+}) released from *C. pyrenoidosa* and total adsorbed Cu^{2+} or MB (C_x) and H^{+} were measured. Cations release due to copper or MB biosorption was calculated by subtracting the concentration of cations released from blanks to the concentration of copper ions or dye measured after biosorption. The ion exchange mechanism is given by the $R_{b/r}$ ratio (Equation 3) (NGAH; HANAFIAH, 2008), where $C_{M^{n+}}$ is the cations concentration (mg.L^{-1}).

$$R_{b/r} = \frac{C_x}{C_{Ca^{2+}} + C_{Mg^{2+}} + \frac{1}{2}C_{Na^{+}} + \frac{1}{2}C_{H^{+}}} \quad (3)$$

4.4.5 Kinetic models

The pseudo first order model of Lagergren (LAGERGREN, 1898) and the pseudo second order model of Ho & McKay (HO; PORTER; MCKAY, 2002), were used to investigate the sorption kinetics, since they are widely used to describe adsorption processes as well as providing important information about the process. The Lagergren model and its linearized form is described by the Equation 4 and Equation 5 respectively, where q_t (mg.g^{-1}) is the biosorption capacity at a given time t (min), $q_{e,calc}$ is the theoretical value of biosorption at equilibrium (mg.g^{-1}) and k_1 (min^{-1}) the pseudo first order rate constant.

$$q_t = q_{e,calc}(1 - \exp(-k_1 t)) \quad (4)$$

$$\ln(q_e - q_t) = \ln(q_{e,calc}) - k_1 t \quad (5)$$

Similarly, the model of Ho & McKay and its linearized form is described by Equation 6 and Equation 7 respectively, where k_2 (g.mg^{-1}.min^{-1}) is the pseudo second order rate constant.

$$q_t = t/(1/k_2 q_{e,calc}^2 + t/q_{e,calc}) \quad (6)$$

$$t/q_t = 1/(k_2 q_{e,calc}^2) + (1/q_{e,calc})t \quad (7)$$

The graph of $\ln(q_e - q_t) - \ln(q_e)$ versus t allows estimating k_1 and the graph of t/q_t versus t allows estimating k_2 and $q_{e,calc}$.

Associated with the pseudo second order model were evaluated the initial adsorption rate h_0 (mg.g^{-1}.min^{-1}) (Equation 8) and the half adsorption time or half-life $t_{0.5}$ (min) (Equation 9), corresponding to the time required for the biosorbent to remove half the amount of copper or MB present in the medium.

$$h_0 = k_2 q_{e,calc}^2 \quad (8)$$

$$t_{0.5} = 1/k_2 q_e \quad (9)$$

4.4.6 Equilibrium isotherms

The Langmuir (LANGMUIR, 1918) isotherm and its linearized form is presented in Equation 10 and Equation 11 respectively, where q_m (mg.g^{-1}) is the maximum theoretical value for the adsorption capacity, C_e is the equilibrium concentration (mg.L^{-1}) and k_l (L.mg^{-1}) is the Langmuir equilibrium constant. The degree of adsorption process development was evaluated by the separation factor (R_L) obtained through the Equation 12 (NASCIMENTO et al., 2014).

$$q_e = q_m k_l C_e/(1 + (k_l C_e)) \quad (10)$$

$$C_e/q_e = (1/k_l q_m) + (1/q_m)c_e \quad (11)$$

$$R_L = 1/(1 + k_l C_0) \quad (12)$$

The Freundlich (FREUNDLICH, 1906) model is given by Equation 13, where k_f (mg$^{1-1/n}$.L$^{1/n}$.g^{-1}) and n are Freundlich equilibrium constants. Its linearized form is presented in Equation 14.

$$q_e = k_f C_e^{1/n} \quad (13)$$

$$log\ q_e = log\ k_f + (1/n)\ log\ C_e \quad (14)$$

Another model used to investigate the adsorption process was proposed by Dubinin-Radushkevich (DUBININ, 1960) (Equation 15) and its linearized form is described by Equation 16. The model allows the understanding of the average energy of adsorption (E) and the interactions involved in the process when correlating the parameter K_{DR}, obtained by the model, through the Equation 17.

$$q_e = q_s \exp\{-K_{DR}[RT \ln(1 + 1/C_e)]^2\} \quad (15)$$

$$\ln q_e = \ln q_s - K_{DR}[RT \ln(1 + 1/C_e)]^2 \quad (16)$$

$$E = 1/\sqrt{2K_{DR}} \quad (17)$$

Where q_s (mg.g^{-1}) is the theoretical isotherm saturation capacity, K_{DR} (mol^2.kJ^{-2}) is the Dubinin-Radushkevich isotherm constant, R (8.314 J.mol^{-1}.K^{-1}) is the ideal gas constant and T (K) the absolute temperature.

The last isotherm model evaluated was proposed by Temkin (TEMKIN, I., 1940) presented in Equation 18 and its linearized form in Equation 19, in which A_t (L.g^{-1}) is the isotherm equilibrium binding constant and b (J.mol^{-1}) is Temkin's isotherm constant related to the adsorption heat.

$$q_e = (RT/b) \ln(A_T C_e) \quad (18)$$

$$q_e = (RT/b) \ln A_t + (RT/b) \ln C_e \quad (19)$$

4.4.7 Thermodynamic parameters

In order to investigate the thermodynamic nature of the processes, the parameters: Gibbs free energy change ($\Delta G°$), enthalpy change ($\Delta H°$) and entropy change ($\Delta S°$) were calculated using Equations 20 and 21 (KOUSHA et al., 2012) where K_d (q_e/C_e) is the distribution coefficient. Experiments were conducted at different temperatures (303; 313; 323 and 333 K) at 250 RPM during 24 h. For the estimation of the parameters involving copper biosorption, the conditions were as follows: 5 mg.L^{-1} of copper ions, 1.5 g.L^{-1} of *C. pyrenoidosa* and pH 6. Regarding the MB biosorption process the conditions employed were: 100 mg.L^{-1} of MB, 2.25 g.L^{-1} of *C. pyrenoidosa* and pH 6

$$\Delta G^o = -RT \ln K_d \quad (20)$$

$$ln\, K_d = \Delta S^o/R - \Delta\, H^o/RT \quad (21)$$

4.4.8 Reliability of model fit

The parameters of the models presented were estimated using a linear and non-linear approach through the Origin 2018 software (OriginLab, USA), with the Levenberg-Marquardt (L-M) algorithm minimizing the chi-square function. The initial values used for non-linear regression were those obtained through linear regression, to optimize and reduce the iterative process.

The validity of the employed models was verified through the correlation coefficient (R^2) (Equation 22) obtained for the regression, besides the parameters sum of error square (SSE) (Equation 23), composite fractional error function ($CFEF$) (Equation 24), and chi-square statistic (χ^2) (Equation 25).

$$R^2 = 1 - \sum(y_{exp} - y_{calc})^2/\sum(y_{exp} - \bar{y}_{exp})^2 \quad (22)$$

$$SSE\ (\%) = \sqrt{\sum \left(y_{exp} - y_{calc}\right)^2/N} \quad (23)$$

$$CFEF = \sum \left(y_{exp} - y_{calc}\right)^2/y_{exp} \quad (24)$$

$$\chi^2 = \sum \left(y_{exp} - y_{calc}\right)^2/y_{calc} \quad (25)$$

In which y_{exp} and y_{calc} corresponds to the experimental and calculated data, respectively, and N to the number of experimental samples. Higher value of R^2, closer to 1, and low values of SSE, $CFEF$ and $\mathcal{X}^2$ indicates a good fit of the applied models.

5. RESULTS AND DISCUSSION

5.1 Chlorella pyrenoidosa Characterization

5.1.1 Scanning electron microscopy and energy dispersive X-ray spectroscopy analysis

Chlorella pyrenoidosa SEM images showed a uniform spherical morphology for the sample (Figure 2), with a particle diameter varying from 14.13 µm to 123.4 µm, with a median of 38.84 µm.

Figure 2 - SEM of *C. pyrenoidosa* sample at 25 keV; magnification 200, with 10 particles marked with their respective diameters.

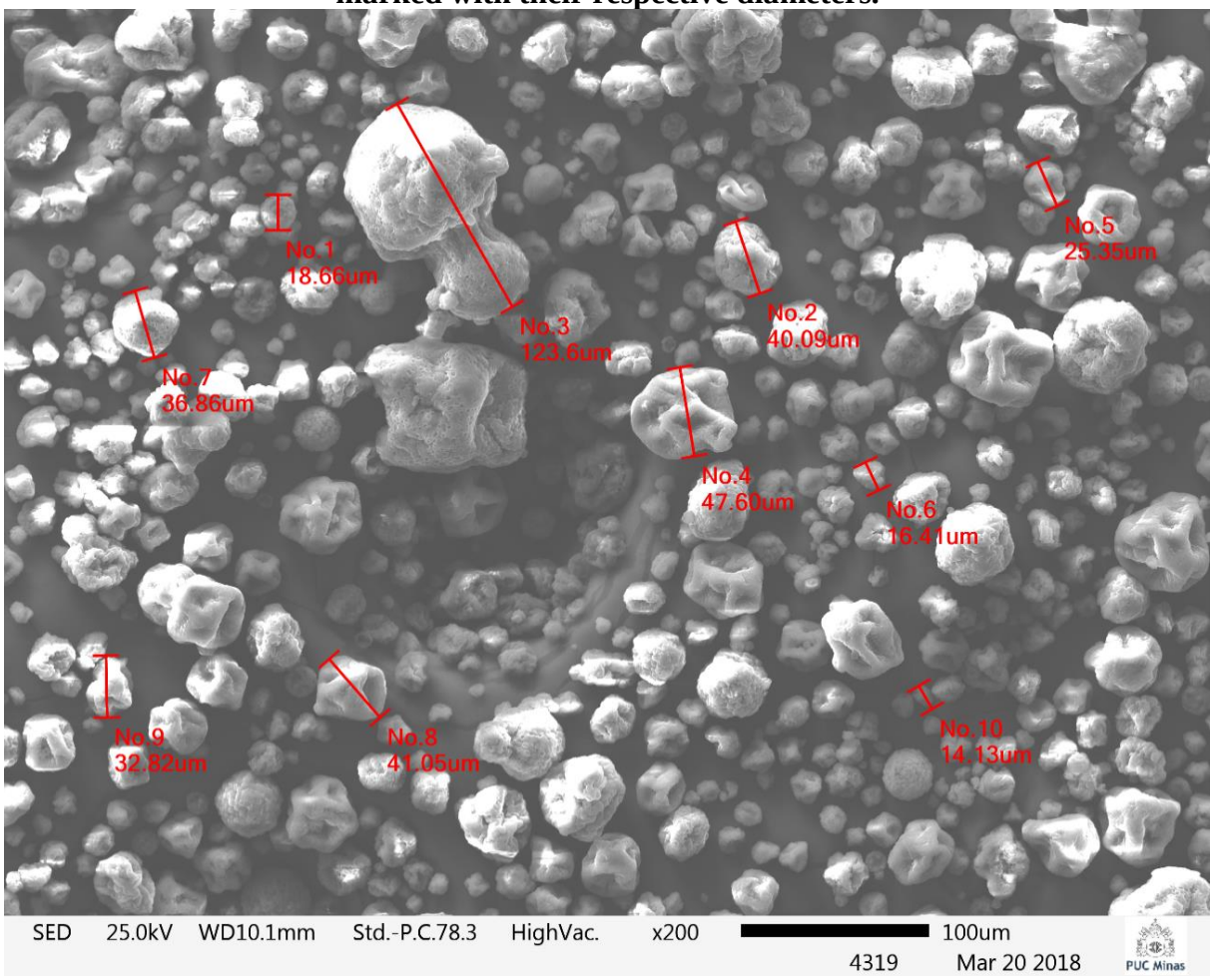

The largest particle (Figure 2, particle Nº 3) with a “mushroom” like morphology was selected for a up close look (Figure 3).

Figure 3 - SEM of *C. pyrenoidosa* sample at 25 keV; magnification 700.

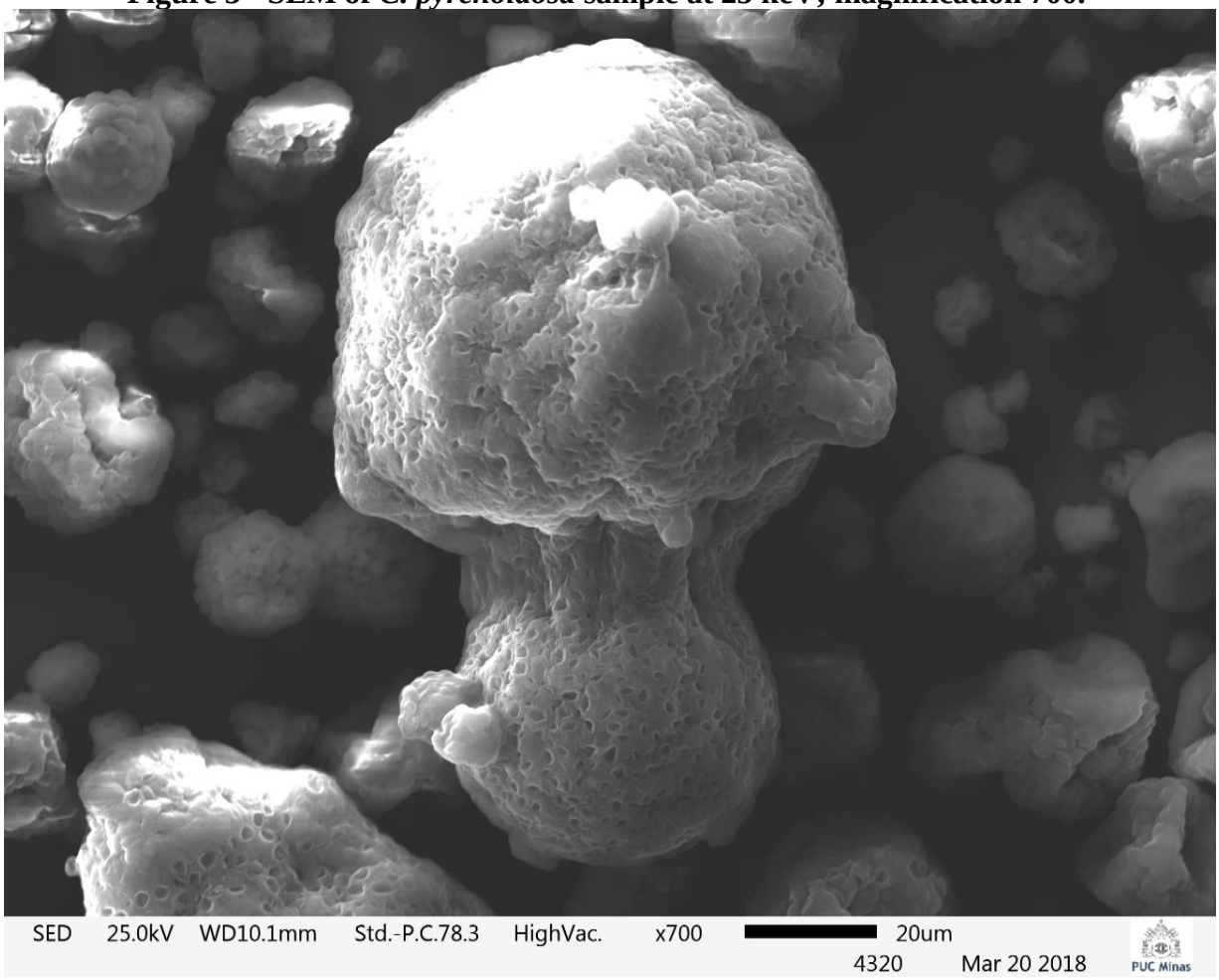

It is possible to observe the presence of pores with an average diameter of 1.868 ± 0.337 µm (Figure 4), classified as macropores by the International Union of Pure and Applied Chemistry (IUPAC). Therefore, the selectivity of the biosorption process should be more associated with the interactions with the surface groups and not with the pore size itself (NASCIMENTO et al., 2014).

Figure 4 - SEM of *C. pyrenoidosa* sample at 25 keV; magnification 2,500.

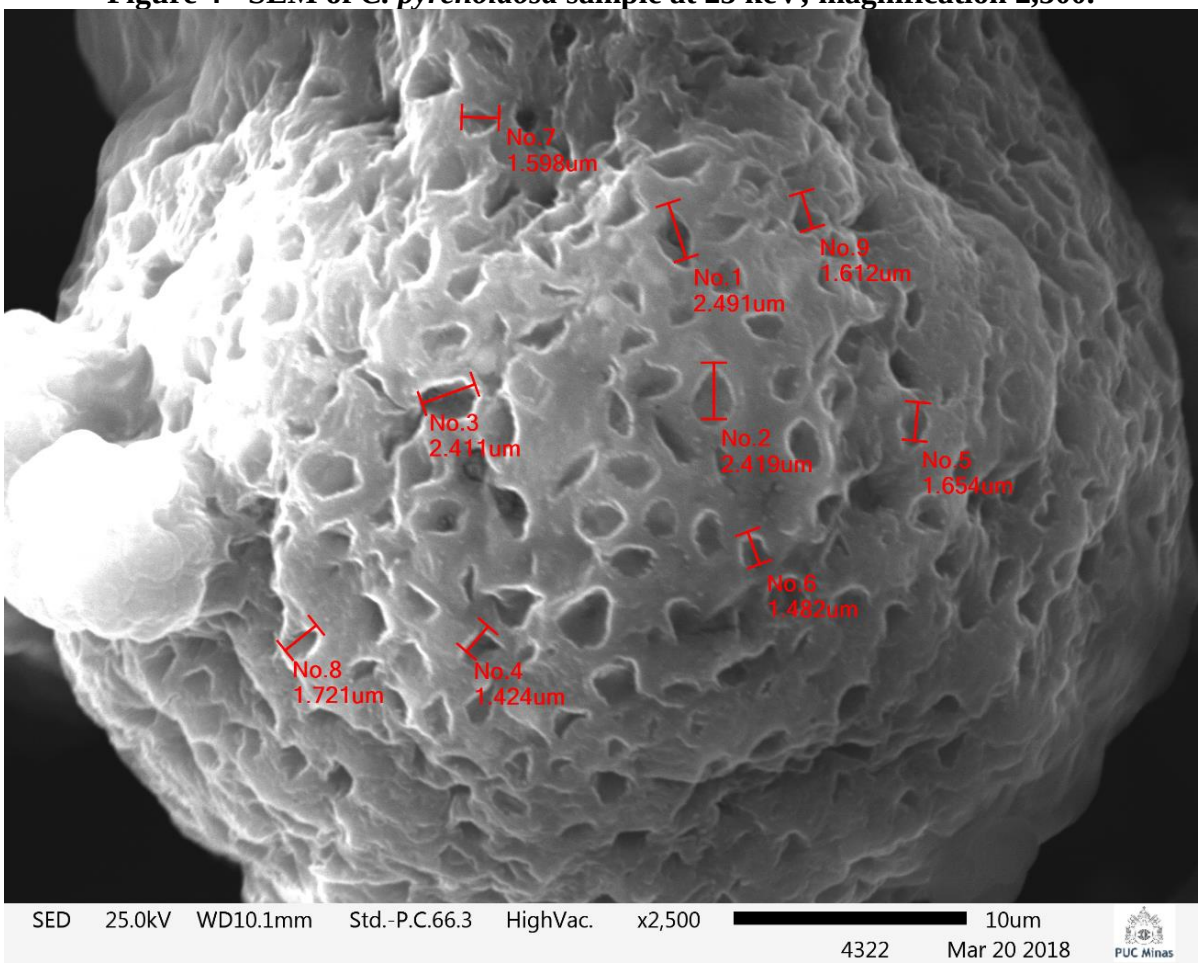

Results obtained through EDS (Figure 5) confirmed the majority of carbon, 68.3%, followed by oxygen with 21.9%, copper 3.9% and other elements that added up to 5.8% of the material composition. Microalgae, when dry, can present 20% of triglycerides, 45% of proteins and 20% of carbohydrates (PHUKAN et al., 2011), which justifies the predominant carbon composition found for the analyzed sample.

Figure 5 - EDS elemental composition analysis of *C. pyrenoidosa* sample.

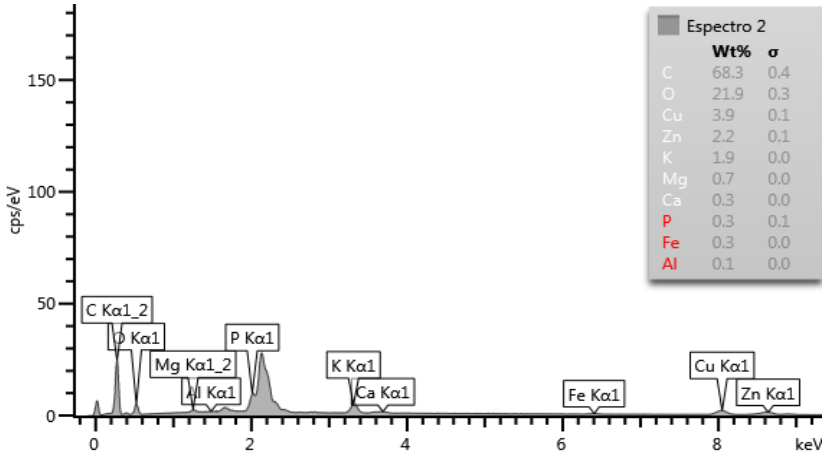

5.1.2 Point of zero charge

For the adsorbent studied, the value of pH_{PZC} obtained was 5.95 (Figure 6). In media with pH lower than pH_{PZC}, the surface charge of the adsorbent is positive and anions adsorption is favored. On the other hand, in media with pH above pH_{PZC} the surface charge of the adsorbent is negative and favors the biosorption of cations (FREITAS; CÂMARA; FREIRE, 2015).

Figure 6 - Point of zero charge (pH_{PZC}) analysis for *C. pyrenoidosa.*

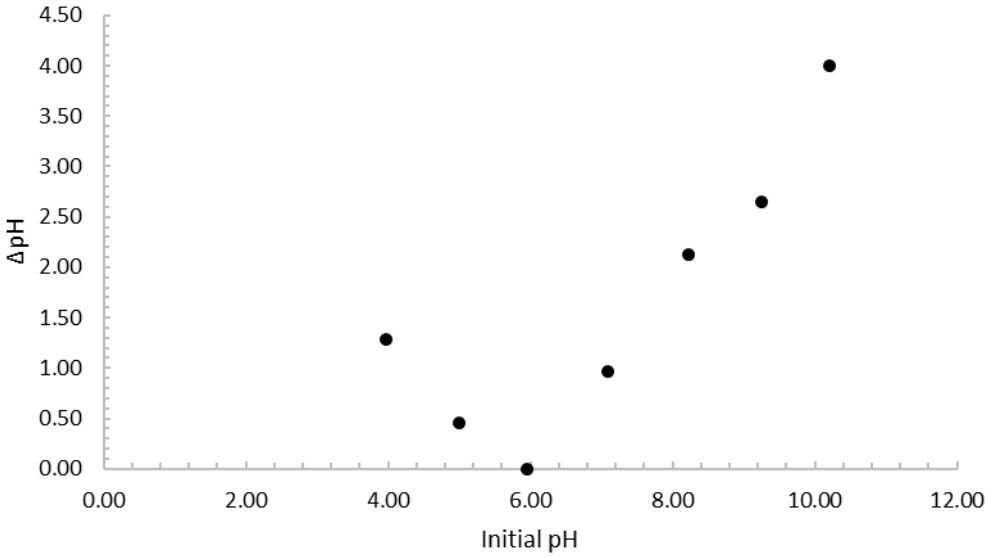

In this sense it is desired to work with solutions with pH> 5.95, where the biosorption of cations is favored, such as MB and copper ions. A comparison with other values of the literature are presented in Table 3.

Table 3 - pH_{PZC} of various biosorbents in the literature.

Biosorbent	pH_{PZC}	Reference
Spirulina platensis	7.00	DOTTO et al., 2012
Chlorella pyrenoidosa	5.95	This study
Sewage sludge	10.17	CHEN et al., 2015
Lobeira Fruit	4-9	ARAÚJO et al., 2018
Modified corn stalk	6.5	CHEN, S. et al., 2012
Coconut shell carbon	7.45	GAUTAM et al., 2014

5.1.3 FTIR analysis

Infrared spectra of *C. pyrenoidosa* is shown in Figure 7 and Figure 8, before and after biosorption processes. The presence of a band at 1643 cm^{-1} results from C=O bond presented in carboxylic acids and derivatives. Between 1800-1500 cm^{-1} the spectra exhibit characteristic bands of proteins (DUMAS; MILLER, 2003), while the bands between 1700-1500 cm^{-1} are specific for primary and secondary amides. The region between 1200-900 cm^{-1} shows a sequence of bands due to vibrations from C-O, C-C, C-O-C and C-O-P bonds and suggest polysaccharides presence (WOLKERS et al., 2004), while the bands in the region of 3100-2800 cm^{-1} resulted of tertiary and secondary carbon bonds suggesting lipids presence (STUART, 2004). A summary of the functional groups observed and its associated wavenumber is shown in Table 4.

Figure 7 - Infrared spectra for *C. pyrenoidosa* before (BA) and after (AA) copper biosorption process.

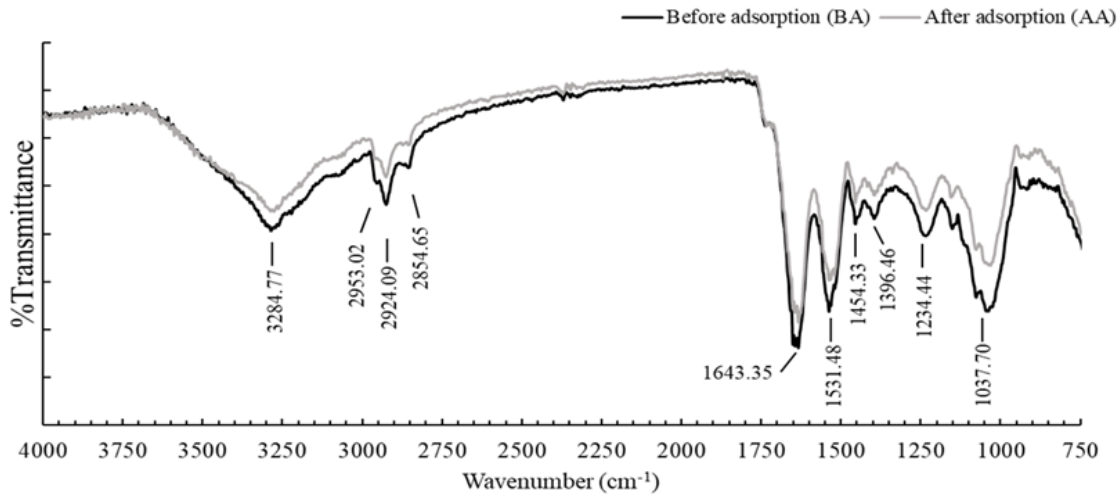

Table 4 - Wavenumber and its associated functional group.

Wavenumber (cm^{-1})		
1200-900	C-O; C-C; C-O-P	Polysaccharides
1643	C=O	Carboxylic acids
1800-1500	NH_2; NH	Proteins
3100-2800	CH_3; CH_2	Lipids

An increase in transmittance was observed after the copper biosorption process (Figure 7), however no apparent change in the FTIR absorption bands was noticed. The fact demonstrated that the copper ions was successfully adsorbed by the microalgae, probably through physical interactions between the ions and the functional groups present. The FTIR analysis is used in several studies (HOU et al., 2012; SHI et al., 2017) to prove the adsorbent

ability to associate with the compounds, whether organic or inorganic. Regarding biosorption process involving heavy metal, Solisio et al. (2017) also observed a reduction on the FTIR absorption bands after mercury biosorption through dry biomass of C. vulgaris.

For both biosorption process there is a similarity in the spectra before and after the process. In the MB biosorption process is possible to denote an increase in transmittance at all peaks (Figure 8), especially the peak in 1643 cm^{-1} due to -C=N- stretching in the poly heterocycles present in the MB (SALAZAR-RABAGO et al., 2017). These results suggests that the MB biosorption onto *C. pyrenoidosa* occurs mainly via physisorption rather than chemisorption, through electrostatic interactions between the MB and the functional groups present on the algae surface (SOLISIO; AL ARNI; CONVERTI, 2017). Similar behaviors were found by Salazar-Rabago et al. (2017) when evaluating the MB biosorption by White Pine (*Pinus durangensis*).

Figure 8 - Infrared spectra for *C. pyrenoidosa* before (BB) and after (AB) methylene blue biosorption process.

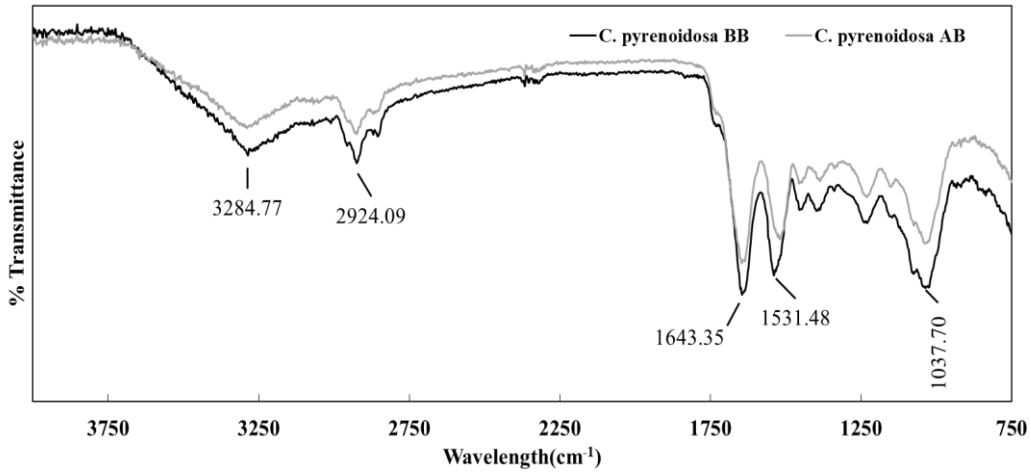

5.1.4 Thermogravimetric analysis

The presence of carbohydrates, proteins and lipids can be determined through TGA and DTG analysis (BACH; CHEN, 2017; RIZZO et al., 2013). Thermogravimetric analysis (Figure 9) showed the first volatilization event occurring between 25 ^{o}C and 150 ^{o}C, associated with the release of water present in the adsorbent, corresponding to 9.63% of the total mass. The second event was responsible for the greater material volatilization (52.28% of the total mass), occurring between 150 ^{o}C and 400 ^{o}C. RIZZO et al. (2013) associated events occurring in this temperature range to the presence of carbohydrates and proteins. The high percentage of these compounds corroborates with the presence of specific functional groups already observed in

the infrared spectra, which favors the interactions between biosorbent and adsorbate, consequently improving the biosorption process. The third and last volatilization event corresponds to 38.09% of the material, occurring between temperatures of 400 ºC to 800 ºC and was associated with the presence of lipids, minerals and residual char (PHUKAN et al., 2011).

Figure 9 - Thermogravimetric analysis for *C. pyrenoidosa* sample (2.725 mg) at a constant nitrogen flow rate.

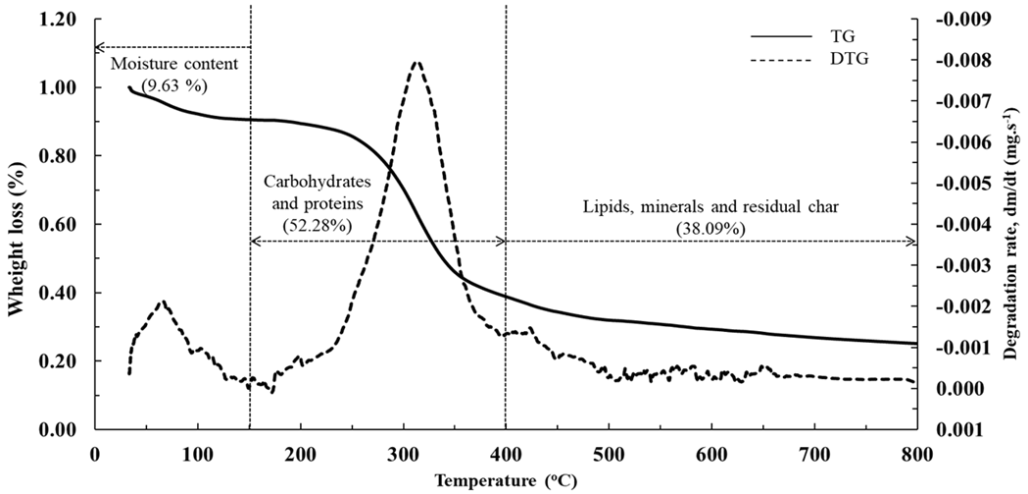

5.2 Adsorption isotherms

The parameters obtained for the Langmuir, Freundlich, Dubinin-Radushkevich and Temkin isotherms are presented in Table 5. In general, it is possible to observe that the values of the error functions namely – R^2, SSE, $CFEF$ and $\mathcal{X}^2$, related to the fit of the isotherm models obtained through the nonlinear approach were smaller than those obtained by the linear approach and as a consequence a great difference in the parameters is observed. Thus evidenced, the use of linear isotherm models can lead to the compromise of the estimate parameters and their interpretations.

The Freundlich model had contrary behavior regarding the biosorption of copper processes in which smaller values of SSE, $CFEF$ and $\mathcal{X}^2$ were observed for the linear approach. For the process evolving the biosorption of MB, smaller values of, SSE, $CFEF$ and $\mathcal{X}^2$ were observed to the linear approach of Dubinin-Radushkevich isotherm , which can be explained by the great similitude between the linear and non-linear equation forms, also observed in Equations 15 and 16, and resulting in a non-reduction on the reliability and model fit parameters chosen (NEBAGHE et al., 2016). Due to this difference between linear and nonlinear models, the use of the linear approach to estimate parameters can lead to data compromise and

subsequent analysis. Therefore, several authors have been using the nonlinear approach to the estimation of kinetic and isothermal parameters related to biosorption (GEORGIN et al., 2018; PERES et al., 2018).

Table 5 - Isotherm parameters obtained using non-linear approach for copper and methylene blue biosorption onto C. *pyrenoidosa*. In parenthesis parameters obtained using linear approach.

Parameter	Copper Biosorption	Methylene Blue Biosorption
	Langmuir	
q_m (mg.g^{-1})	11.877 (10.395)	114.153 (113.636)
k_l (L.mg^{-1})	0.125 (0.504)	0.296 (0.304)
$R_{L,máx}$	0.227	0.058
$R_{L,min}$	0.048	0.024
R^2	0.995 (**0.997**)	0.993 (**0.999**)
SSE (%)	**0.102** (0.664)	**1.052** (1.125)
$CFEF$	**0.007** (0.387)	**0.124** (0.137)
$\mathcal{X}^2$	**0.007** (0.501)	**0.126** (0.138)
	Freundlich	
k_f (mg$^{1-1/n}$.L$^{1/n}$.g^{-1})	3.188 (5.226)	45.023 (41.467)
n	3.173 (5.189)	3.965 (3.478)
R^2	0.965 (**0.989**)	0.910 (**0.914**)
SSE (%)	0.283 (**0.166**)	**2.136** (2.297)
$CFEF$	0.056 (**0.018**)	1.976 (**1.973**)
$\mathcal{X}^2$	0.056 (**0.018**)	**1.897** (1.949)
	Dubinin-Radushkevich	
K_{DR} (mol^2.kJ^{-2})	0.015 (0.220)	1.126 (0.991)
q_s (mg.g^{-1})	5.782 (8.423)	93.865 (91.814)
E (kJ.mol^{-1})	5.834 (1.507)	0.666 (0.710)
R^2	0.841 (**0.871**)	0.875 (**0.902**)
SSE (%)	**0.604** (0.871)	2.364 (**2.349**)
$CFEF$	**0.272** (0.460)	2.439 (**2.365**)
$\mathcal{X}^2$	**0.257** (0.463)	2.443 (**2.400**)
	Temkin	
b (kJ.mol^{-1})	0.991 (1.748)	0.117 (0.117)
A_t (L.g^{-1})	1.358 (32.216)	4.680 (4.679)
R^2	**0.988 (0.988)**	**0.958 (0.958)**
SSE (%)	0.169 (**0.166**)	**1.747** (1.748)
$CFEF$	**0.018** (0.021)	**0.805** (0.806)
$\mathcal{X}^2$	**0.019** (0.020)	**0.807 (0.807)**
	Maximum experimental biosorption capacity	
$q_{e,max}$ (mg.g^{-1})	12.580	101.747

For both biosorption process the Langmuir model was the on which best fit the obtained data, suggesting that the process is limited to the formation of a monolayer. On either copper or MB process, the range obtained for the separation factor suggests a favorable process ($0<R_L<1$) in which small amounts of the biosorbent are able to adsorb high amounts of copper ions (FU et al., 2015).

In the other hand, lower values of R^2 were observed for Dubinin-Radushkevich model, in addition to the high values for SSE, $CFEF$ and χ^2 for either copper or MB biosorption process, which can be explained by the model limitation of to consider the system complexity, such as pH and the distribution of the adsorbate molecules, being more suitable to describe the adsorption in gaseous medium. Nevertheless, the model allows the distinction between chemical and physical adsorption processes when evaluating parameter E. For values smaller than 8 kJ.mol^{-1} there is a predominance of physical interaction, while values between 8-16 kJ.mol^{-1} suggest chemical interaction (MITROGIANNIS et al., 2015). For the present study, the E value obtained for both cases suggests that the adsorbate and adsorbent interaction is essentially due to physical attractions.

Temkin model satisfactorily fitted the copper biosorption process, where the value of the constant related to the heat of biosorption, b (0.991 kJ.mol^{-1}), reinforces the physical biosorption mechanism already indicated by the Dubinin-Radushkevich isotherm. Since the Temkin model presented a high value of R^2 and low value of SSE, $CFEF$ and χ^2 it can be stated that the heat of biosorption of all molecules in a layer would decrease linearly rather than logarithmically with the coverage degree (ARAÚJO et al., 2018). A similar conclusion can be obtained for the biosorption of MB, as the value of b (0.117 kJ.mol^{-1}) obtained also suggests a physical biosorption mechanism as previously indicated by the Dubinin-Radushkevich isotherm.

As observed in Table 5, and also in Figure 10, the maximum adsorption capacity for copper (12.580 mg.g^{-1}) was lower than the maximum adsorption capacity of methylene blue (101.747 mg.g^{-1}). The adsorption capacity differences of metal and dye uptake are due to the properties of each adsorbent such as structure, functional groups and surface area and the experimental condition. Similar behavior was observed by Han et al. (2010), Zhang et al. (2014) and Wu et al. (2009), in which the biosorbent presented a higher adsorption capacity for dyes.

Figure 10 - Biosorption equilibrium for copper and methylene blue.

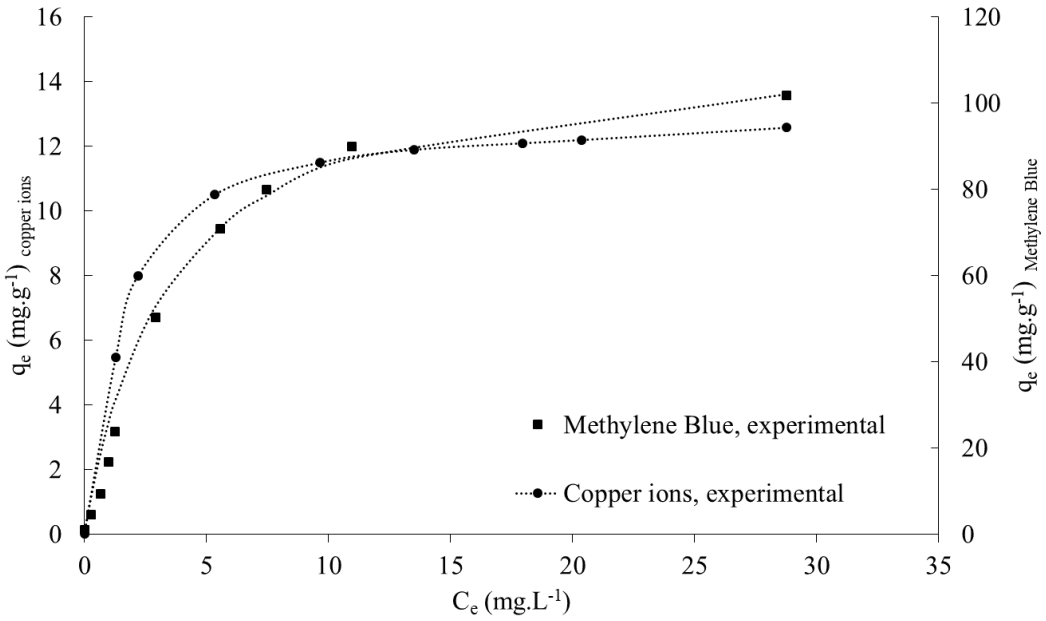

The adsorption capacity obtained in this study was compared with other published articles. Table 6 provides a summary of the comparison.

Table 6 - Comparison of the maximum monolayer of copper and methylene blue biosorption onto various biosorbents.

Copper Biosorption		
Biosorbent	q_e (mg.g^{-1})	Reference
Xylaria sp. (fungi)	73.26	(WONG et al., 2018)
Rhodococcus erythropolis	68.03	(BALTAZAR et al., 2018)
Pine cone shell	6.52	(MARTÍN-LARA et al., 2016)
Pine bark	6.05	(RONDA et al., 2014)
Olive stone	1.34	(RONDA et al., 2014)
Dried *C. pyrenoidosa*	12.58[a]	This study
Diaporthe sp. (fungi)	72.65	(WONG et al., 2018)
Ceriporia lacerata	7.76	(LI et al., 2015)
Methylene Blue Biosorption		
Biosorbent	q_e (mg.g^{-1})	Reference
Modified pine cone	142.24[a]	(YAGUB; SEN; ANG, 2014)
Modified saw dust	111.46[a]	(ZOU et al., 2013)
Pinus durangensis sawdust	102	(SALAZAR-RABAGO et al., 2017)
Dried *C. pyrenoidosa*	101.75[a]	This study
Tea waste	85.16	(UDDIN et al., 2009)
Dried *Arthrospira platensis*	82.95[a]	(MITROGIANNIS et al., 2015)
Platanus orientalis leaf powder	68.95[a]	(PEYDAYESH; RAHBAR-KELISHAMI, 2015)
Activated carbon from *Ficus carica*	47.62	(PATHANIA; SHARMA; SINGH, 2017)

[a] maximum experimental adsorption capacity

5.3 Kinetic Studies

The parameters obtained from the kinetic models, namely the pseudo first order and the pseudo second order, are shown in Table 7.

Table 7 - Kinetics parameters obtained using non-linear approach for copper and methylene blue biosorption onto *C. pyrenoidosa*. In parenthesis parameters obtained using linear approach.

Parameters	Copper	Methylene Blue
Pseudo First order		
k_1 (min^{-1})	0.373 (0.021)	2.889 (0.072)
$q_{e,calc}$ ($mg.g^{-1}$)	2.635 (2.802)	41.776 (3.093)
R^2	**0.989** (0.888)	**0.993** (0.817)
SSE (%)	**0.085** (0.737)	0.957 (**0.751**)
$CFEF$	**0.025** (0.481)	**0.303** (6.816)
$\mathcal{X}^2$	**0.025** (0.396)	**0.295** (9.702)
Pseudo Second order		
k_2 ($g.mg^{-1}.min^{-1}$)	0.317 (0.196)	0.161 (0.161)
$q_{e,calc}$ ($mg.g^{-1}$)	2.738 (2.793)	42.701 (42.735)
h ($mg.g^{-1}.min^{-1}$)	2.379 (1.528)	294.238 (294.118)
$t_{0.5}$ (min)	1.151 (1.828)	0.145 (0.145)
R^2	0.997 (**0.999**)	**0.999 (0.999**)
SSE (%)	**0.044** (0.195)	0.135 (**0.075**)
$CFEF$	**0.008** (0.049)	0.004 (**1.83E-5**)
$\mathcal{X}^2$	**0.008** (0.046)	0.004 (**1.83E-5**)
Maximum experimental biosorption capacity		
$q_{e,max}$ ($mg.g^{-1}$)	2.802	42.712

Similarly to the estimation of the isotherms parameters, the error functions values for the nonlinear pseudo first order model was smaller than that obtained by the linear model, except to the SSE (%) value for the MB biosorption process. The inverse happened to the pseudo second order model, in which smaller values of R^2, SSE, $CFEF$ and $\mathcal{X}^2$ were obtained.

The pseudo second order model proposed by Ho & McKay presented a higher R^2 when compared to the one related to the other pseudo first order model for the copper biosorption process. Moreover, the proximity of $q_{e,calc}$ (2.738 $mg.g^{-1}$) and $q_{e,exp}$ (2.802 $mg.g^{-1}$), and the lower values obtained for SSE, $CFEF$ and $\mathcal{X}^2$, suggest that this process follow a pseudo second order model. A similar conclusion can be made for the MB biosorption process since a high value of R^2, in addition to the low values of SSE, $CFEF$ and $\mathcal{X}^2$ and the proximity between $q_{e,calc}$ (41.776 $mg.g^{-1}$) and $q_{e,exp}$ (42.712 $mg.g^{-1}$), suggested a process governed by a pseudo-second order model. Several studies (KHATAEE; VAFAEI; JANNATKHAH, 2013;

MITROGIANNIS et al., 2015) have reported that the pseudo-second order model presents a good adjustment of data when compared to the pseudo first order model, therefore, it is widely used in the study of the kinetics of biosorption of dyes in solution.

When the equilibrium concentration was evaluated throughout the biosorption process (Figure 11 and Figure 12), it could be observed that the kinetics was favorable in both media, reaching the equilibrium in approximately 30 minutes after the beginning of the process. Biosorption of MB had a higher value of initial adsorption rate (h), which can also be observed in Figure 12 as the biosorption capacity was more significant for the first minutes. The same process also presented half biosorption time value ($t_{0.5}$), of 0.145 min, 87% lower than that obtained for the copper biosorption process. This phenomenon can be also visualized in Figure 12, in which a greater initial adsorption capacity for the MB biosorption process is observed.

Figure 11 - Experimental values and pseudo first order kinetic model fitting for copper and methylene blue biosorption by *C. pyrenoidosa*.

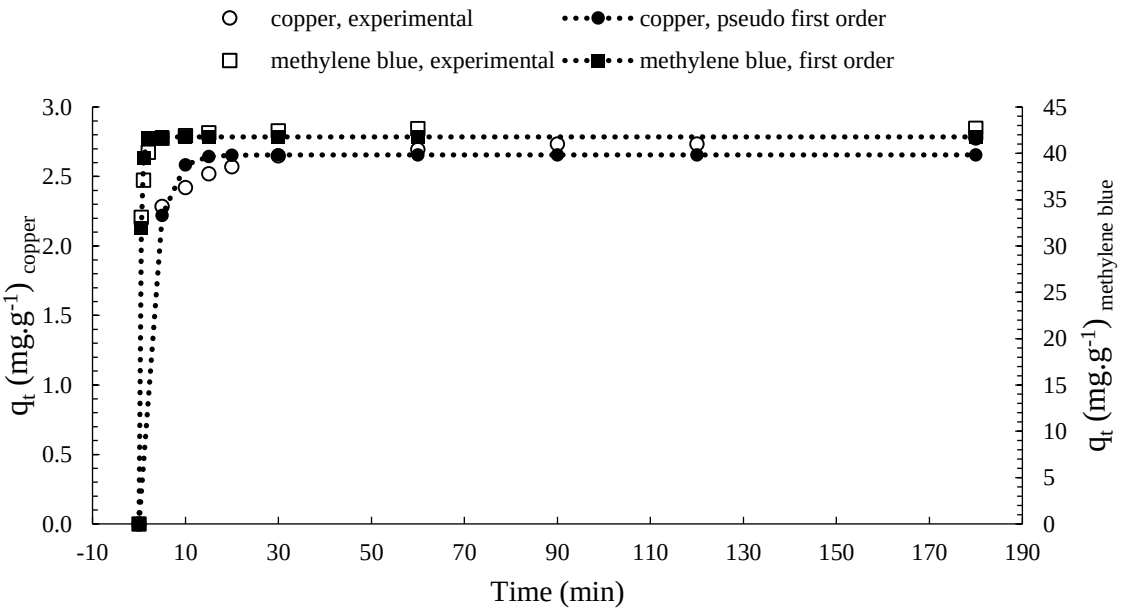

Figure 12 - Experimental values and pseudo second order kinetic model fitting for copper and methylene blue biosorption by *C. pyrenoidosa*.

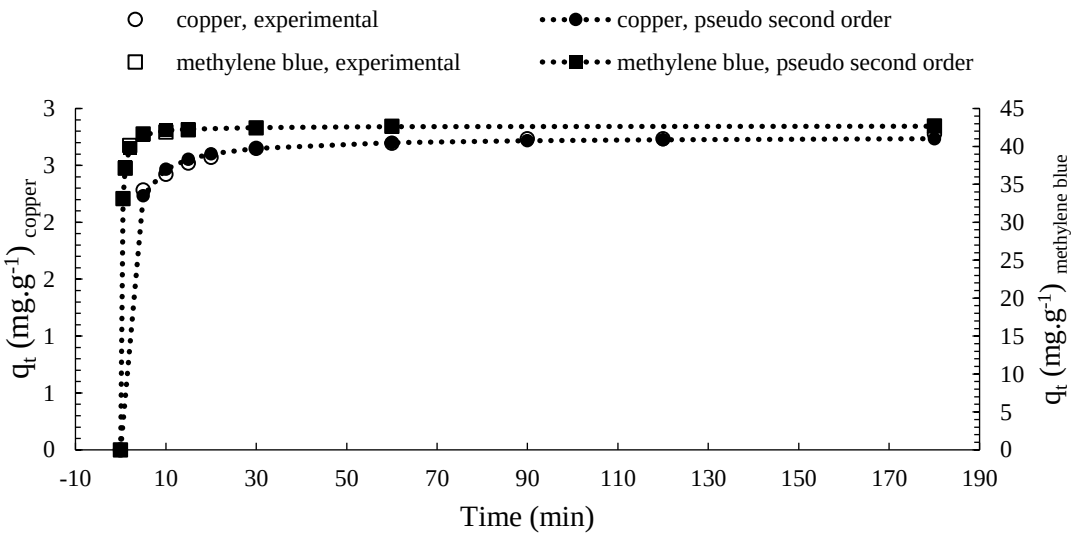

5.4 Thermodynamic studies

In the thermodynamic data of the copper biosorption process (Table 8) the negative values of $\Delta G°$ indicated the spontaneous nature of the process and its feasibility for the temperature range evaluated. Moreover, the increase in temperature resulted in a slightly decrease on Gibbs free energy change, being propitious for the biosorption process (Figure 13). The positive value observed for $\Delta H°$ indicates an endothermic process and its low value suggests a predominance of Van der Waals interactions, typical of a physical adsorption process (FU et al., 2015), which corroborates the results observed by the infrared spectra and isotherm parameters. Furthermore, the increase in temperature of the system may lead to an increase of active sites for the copper biosorption on the adsorbent surface and can also lead to the boundary layer reduction surrounding the adsorbent, in both cases the consequence is the increase removal efficiency, thus characterizing the endothermic nature of the process (KHATAEE; VAFAEI; JANNATKHAH, 2013; TAN et al., 2011). The positive value of the enthalpy change could be explained by observing that the bonding energy between the solvated copper ions and the water are greater than the binding energy between these ions and the surface of the adsorbent. Meanwhile, the positive value of $\Delta S°$ indicated an increase in randomness at aqueous-solid interface during the sorption of copper ions onto the sites of the adsorbent. This entropy increase may be due to the greater movement freedom of copper ions on the surface of *C. pyrenoidosa* when compared to its solvated state by water molecules in solution.

Table 8 - Thermodynamic parameters for the biosorption of copper ions and methylene blue onto *C. pyrenoidosa*.

	T (K)	ΔG° (kJ.mol^{-1})	ΔH° (kJ.mol^{-1})	ΔS° (kJ.mol^{-1}.K^{-1})	R^2	SSE (%)	$CFEF$	χ^2
Copper Ions	303	-3.844 ± 0.130	48.317 ± 2.867	0.172 ± 0.009	0.993	0.0540	0.0056	0.0057
	313	-5.565 ± 0.040						
	323	-7.285 ± 0.050						
	333	-9.006 ± 0.141						
MB	304	-6.183 ± 0.024	-29.168 ± 0.525	-0.076 ± 0.002	0.999	0.0896	0.0003	0.0003
	314	-5.427 ± 0.008						
	326	-4.520 ± 0.011						
	334	-3.916 ± 0.024						

(Mean ± Standard deviation, N=3)

Regarding MB biosorption the process was spontaneous in the experimental conditions as indicated by the negative values of $\Delta G°$ (Table 8) suggesting that the system required no energy input from outside (MITROGIANNIS et al., 2015). Similar results were found by Fan *et al*. (2017) and Vaz et al. (2017) when evaluating the $\Delta G°$ value for MB adsorption using other adsorbents. Besides, the $\Delta H°$ negative value demonstrated that the MB biosorption is exothermic, for this reason, an increase in the operating temperature disadvantages the biosorption process as observed in Figure 13.

Figure 13 - Gibbs free energy variation with the temperature of the system for biosorption of copper ions and MB onto *C. pyrenoidosa*.

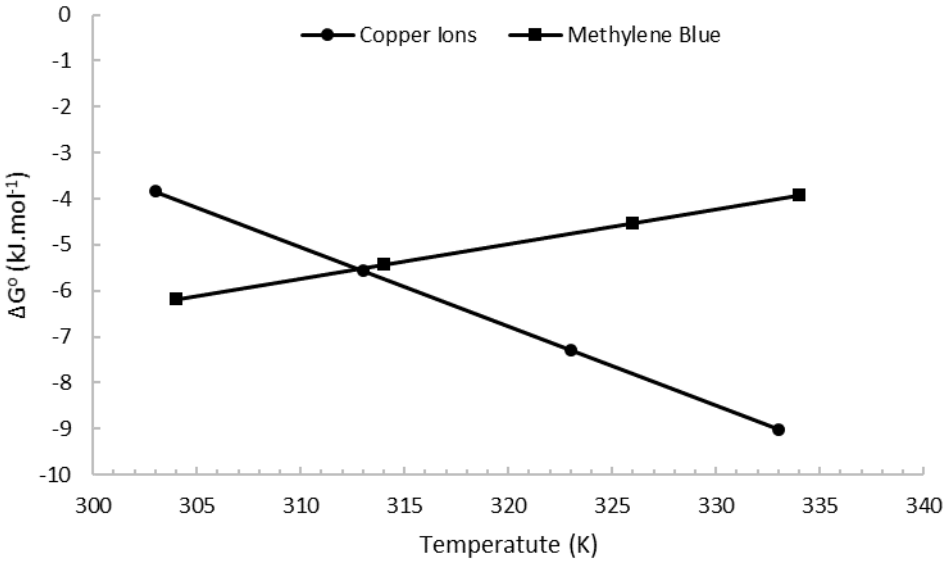

Furthermore, the $\Delta H°$ magnitude can be used to evaluate the type of interaction that occurs between the adsorbent and the adsorbate. Values of $\Delta H°$ > 80 kJ.mol^{-1} suggest interactions in the order of chemical bonds (chemisorption), whereas the physical adsorption

has lower values. Values in the range of 4-10 kJ.mol^{-1} indicate van der Waals type interactions and values $\Delta H°$ < 30 kJ.mol^{-1} indicate hydrogen bonding type interactions (CARDOSO et al., 2012). In this study, $\Delta H°$ values for both adsorbate (-29.168 kJ.mol^{-1} for MB biosorption and 48.317 kJ.mol^{-1} for copper ions biosorption) indicated a physical biosorption mechanism, with interactions in the order of hydrogen bonds. Hassan & Elhadidy (2017) evaluated the value of $\Delta H°$ for the adsorption of MB by activated carbons from waste carpets and found a similar value of -29.744 kJ.mol^{-1}. Mitrogiannis et al. (2015) found a value of -28.32 kJ.mol^{-1} for the biosorption of MB by *Arthrospira platensis*. The $\Delta S°$ value found for MB biosorption was -0.076 kJ.K^{-1}.mol^{-1}. The $\Delta S°$ value obtained was negative and low, indicating reduction disorder in the solid-liquid interface during the biosorption process. As this value was low, it can be inferred that the $\Delta H°$ value contributes more to the $\Delta G°$ negative values. A similar behavior was found by Mitrogiannis et al. (MITROGIANNIS et al., 2015) who evaluated the MB biosorption process by *A. platensis* and found a value a $\Delta S°$ of -0.011 kJ.K^{-1}.mol^{-1}.

5.5 Statistical analysis

5.5.1 Copper ions biosorption

The values for the copper removal percentage obtained experimentally and those obtained by the model are shown in Table 9.

Table 9 - Actual and predicted values for the copper percentage removal.

Run Order	Actual[a] (%)	Predict	Residual
1	69.15 ± 6.94	70.81	-1.66
2	50.43 ± 1.52	51.47	-1.04
3	76.17 ± 8.27	75.13	1.04
4	55.33 ± 4.91	53.67	1.66
5	70.80 ± 6.70	69.98	0.82
6	32.37 ± 4.99	32.17	0.2
7	81.66 ± 2.37	81.87	-0.2
8	78.05 ± 2.18	78.88	-0.82
9	45.12 ± 1.34	44.29	0.83
10	43.52 ± 5.15	45.39	-1.87
11	73.29 ± 2.64	71.43	1.86
12	76.01 ± 4.59	76.85	-0.83
13	73.18 ± 6.97	73.1	0.08
14	73.09 ± 3.31	73.1	-0.01
15	73.03 ± 4.38	73.1	-0.07

[a]Mean ± standard deviation (N=3)

Linear, two-factor interaction (2FI), quadratic and cubic models were used to adjust the experimental data to obtain the appropriate regression equations. To determine the model suitability describing the copper removal by *C. pyrenoidosa* the sequential sum of squares and the summary of the model statistics were analyzed (Table 10). The results of the sequential sum of squares of the models indicated that the 2FI and linear model did not provide a good description of the experimental data, as it was not statistically significant (p>0.05) and had low R^2 respectively. From the summary statistics of the model it can be seen that for the quadratic model the predicted R^2 agrees with the adjusted R^2, in addition, this model obtained the highest values of R^2. For these reasons the quadratic model, described in terms of the codded variables by Equation 26, was selected as the most appropriate model for later analysis.

Table 10 - Adequacy of the model tested for copper ions biosorption.

Source	Sum of squares	df[a]	Mean square	F value	p value
Sequential sum of squares					
Linear	2570.56	3	856.85	14.15	0.0004
2FI	308.90	3	102.97	2.31	0.1532
Quadratic	339.49	3	113.16	32.37	0.0011
Cubic	17.47	3	5.82	1021.67	0.0010
Source	Std. Dev.	Predicted R^2	Adjusted R^2	R^2	PRESS[c]
Model Summary Statistics					
Linear	7.78	0.7943	0.7381	0.6237	1218.01
2FI	6.68	0.8897	0.807	0.6828	1026.51
Quadratic	1.87	0.9946	0.9849	0.9136	279.56
Cubic	0.0755	[b]	1	1	[d]

[a]Degrees of freedom. [b]Case with leverage of 1.0000, Pred. R^2 statistic is not defined. [c]Predicted residual sum of squares. [d]Not defined.

$$\%Removal = 73.1 - 10.2 * A + 1.63 * B + 14.65 * C - 0.53 * AB + 8.705 * AC + 1.08 * BC - 2.05 * A^2 - 8.28 * B^2 - 5.33 * C^2 \quad (26)$$

In which A corresponds to copper concentration (mg.L^{-1}), B to pH and C to biosorbent concentration (g.L^{-1}).

The ANOVA results for the quadratic equation presented in Table 11 suggests that the model is as statistically significant (p<0.05). The sum of squares (SS) of each factor quantifies its importance in the process and as the value of the SS increases, the significance of the corresponding factor in the process also increases (REGTI et al., 2017).

Table 11 - Analysis of variance (ANOVA) for the obtained regression model for the copper ions removal.

Source	SS	df	Mean Square	F value	p value Prob. > F
Model	3218.95	9	357.66	102.29	< 0.0001
A	832.32	1	832.32	238.05	< 0.0001
B	21.26	1	21.26	6.08	0.0568
C	1716.98	1	1716.98	491.07	< 0.0001
AB	1.12	1	1.12	0.3214	0.5953
AC	303.11	1	303.11	86.69	0.0002
BC	4.67	1	4.67	1.33	0.3002
A^2	15.48	1	15.48	4.43	0.0893
B^2	253.29	1	253.29	72.44	0.0004
C^2	104.99	1	104.99	30.03	0.0028
Residual	17.48	5	3.5		
Lack of Fit	17.47	3	5.82	1021.67	0.001
Pure Error	0.0114	2	0.0057		
Std. Dev.	1.87		Adjusted R^2	0.9849	
Mean	64.75		Predicted R^2	0.9136	
C.V. %	2.89		Adeq. Precision	32.553	
R^2	0.9946				

A: copper concentration (mg.L^{-1}); B: pH; C: biosorbent concentration (g.L^{-1}).

In this study, B, AB, BC, and A^2 were not significant factors. On the contrary A, C, AC, B^2 and C^2 were significant. The resulting effects and significance of each factor can be observed through a Pareto chart (Figure 14(a)). In this graph, it is possible to highlight the significant factors, which exceeded the vertical line of p = 0.05. It is also possible to observe the relation and the magnitude of the influence of these factors, denoted by the signal and the value on each horizontal bar.

Given that the adjusted and predicted R^2 for the complete model (Equation 26) were high and concordant with each other (difference < 0.2) the use of a reduced model is not justified, since the number of parameters in the complete model did not influence the adjusted R^2. This is an indicative that the model it is not over-fit to the given data (TERBLANCHE et al., 2017). Furthermore, the elimination of non-significant terms from the model would reduce the dimensionality and thus the accuracy of the response surface (LAMBROPOULOU et al., 2017).

Adequate precision is a measure of the expected response range relative to the associated error, in other words, a signal-to-noise ratio. Its desired value is 4 or more (SOLTANI et al., 2013), in this study the ratio of 32.55 indicated a suitable signal. The low coefficient of variation

(2.89%) indicated that the deviations between the experimental and predicted values are low and not only showed a high degree of accuracy, but also presented good reliability in the experiments performed, as stated by PRAKASH MARAN et al. (2013). The lack of fit was significant, which did not invalidate the model for predictive purposes, since the equation presented a high value R^2 and the analysis of variance presented the model as significant (p<0.001) (CAZETTA et al., 2005).

Figure 14 - (a) Pareto chart of the standardized effects. (b) A residual plot showing the deviation of predicted values from experimental values for each case number. (c) Normal plot of residuals. (d) Plot of the experimental and predicted responses.

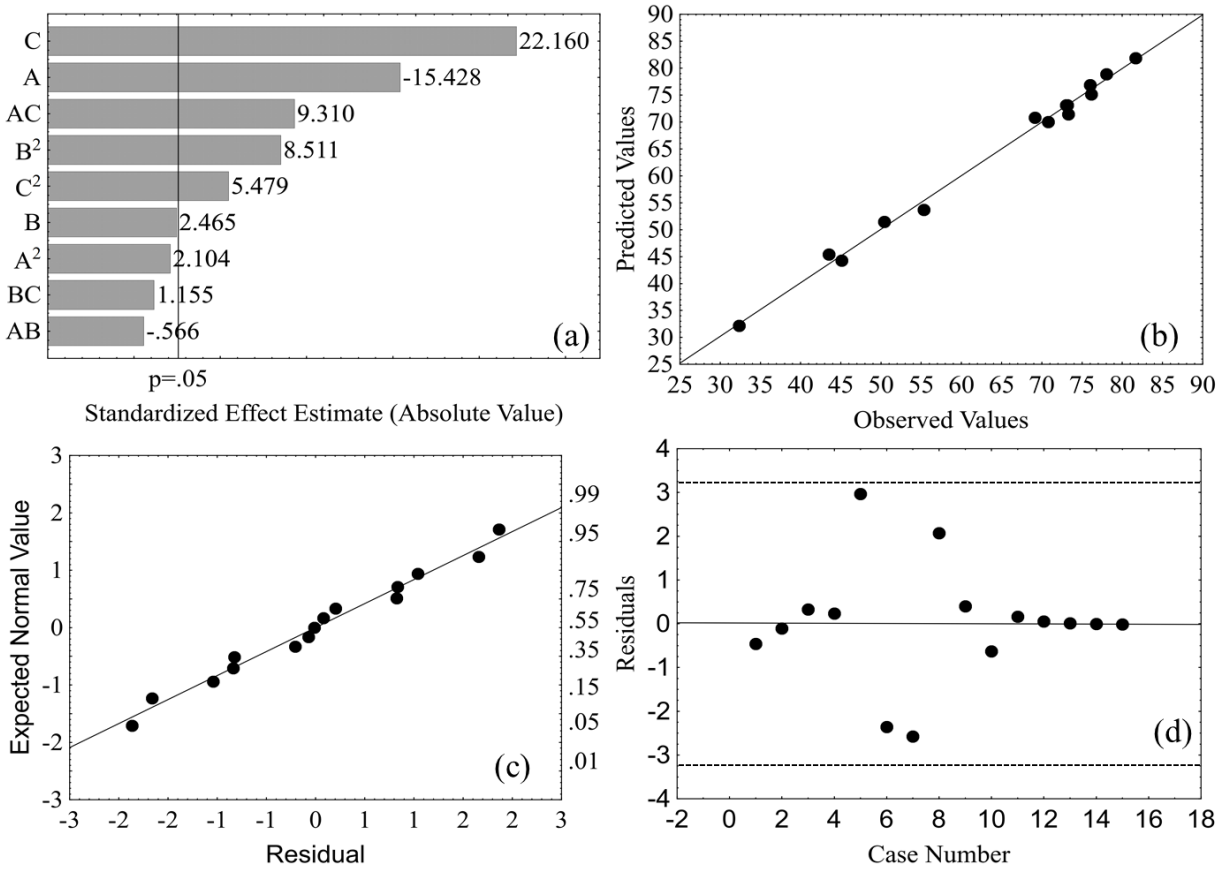

The data were also analyzed to verify the correlation between the experimental copper removal values (%) and the values predicted by the model as shown in Table 9. It can be seen in Figure 14(b) that the data points in the graph are evenly distributed along the straight line, indicating a good relationship between the experimental and predicted values, this result also suggests that the quadratic model is suitable for predictive purposes. In Figure 14(c) the residual values are normally distributed, since these falls close enough to the straight line of the normal probability plot. It is expected an approximation of randomly distributed points, characterizing

a constant variance of the errors (CALADO; MONTGOMERY, 2003). This behavior is observed in Figure 14(d) for the quadratic model obtained.

5.5.1.1 Effect of various parameters on copper ions removal efficiency

The best way to identify the relationship between the factors and response is to evaluate response surfaces as a function of two factors, keeping the other factor at a certain level, usually the central one (MOURABET et al., 2012). It can be observed in Figure 15(a) that in regions of pH 6 and lower concentrations of metal in the system higher percentages of removal are obtained. In contrast, in extreme regions of pH (8 and 4) and high concentration of metal (10 mg. L^{-1}) lower removal percentages are obtained.

Figure 15 - Three-dimensional response surface for effect of independent variables on %Removal. In (a) the biosorbent concentration is fixed, in (b) the pH and (c) the copper concentration, all fixed at their intermediate levels.

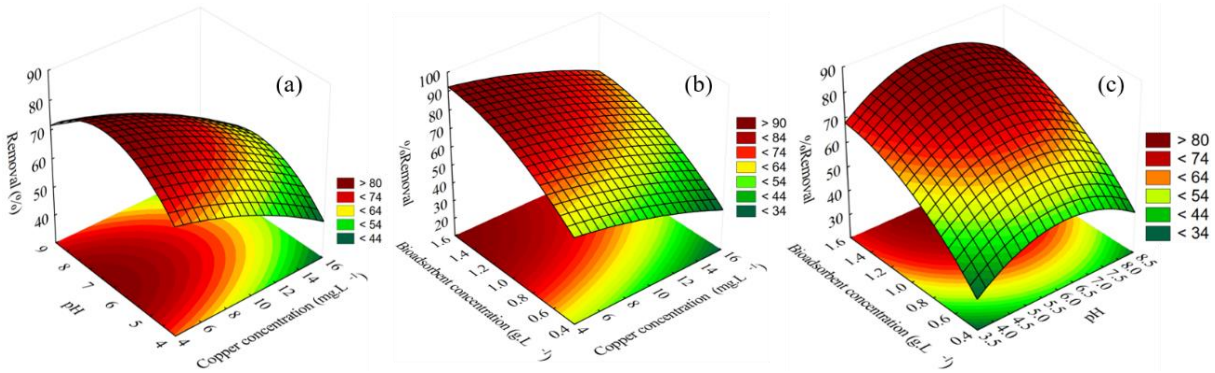

A large area with high removal percentage was observed in Figure 15(b) when the pH was fixed at its central point (pH = 6), but in regions with high concentrations of metal (15 mg.L^{-1}) and low concentrations of algae (0.5 g.L^{-1}) this percentage drops, in contrast, when the system has low concentrations of algae (0.5 g.L^{-1}) there is a great influence of metal concentration.

When the interaction between biosorbent concentration and pH is evaluated, Figure 15(c), a region of high removal percentage occurs when the pH is presented at its intermediate level (6) and the algae concentration at higher levels (1.5 g.L^{-1}). There is no significant difference in the percentage of removal when the pH is in extreme bands (4 and 8) and the algae concentration is lower (0.5 g.L^{-1}), when this concentration becomes higher (1.5 g.L^{-1}) the removal is maximum when the pH is 6.

5.5.1.2 Process optimization

The surface plots and contour plots (surface projection on the x-y plane) shown in Figure 15 are part of a parabolic cylinder, exhibiting a minimum and maximum crest in the investigated domain, thus indicating the presence of a maximum point of copper removal from an aqueous medium by *C. pyrenoidosa*. The desirability function approach was originally introduced by Harrington (1965) and this technique was used in this study for the simultaneous determination of optimum settings of input variables that can determine optimum performance levels for the response.

The parameters used for optimization of the system to find this maximum point and the solution of this optimization problem is presented in Table 12.

Table 12 - Optimization parameters and results obtained for the copper ions biosorption process by *C. pyrenoidosa*.

			First case		Second case	
	Lower limit	Upper limit	Goal	Result	Goal	Result
A: Copper ions ($mg.L^{-1}$)	5	15	in range	5	maximize	10.438
B: pH	4	8	in range	6.335	in range	6.229
C: Biosorbent ($g.L^{-1}$)	0.5	1.5	in range	1.286	minimize	1.145
Removal (%)	32.37	100	maximize	83.141	maximize	76.340

The maximum removal percentage was 83.14% for a metal concentration of 5 $mg.L^{-1}$ with a system pH of 6.33, which is in agreement with the pH_{PZC} found in this study, and an algae concentration of 1.28 $g.L^{-1}$.

In order to obtain the highest removal percentage with a higher initial concentration of metal and a reduction of the algae concentration, a new optimization was elaborated with the parameters and solution in Table 12. It is possible to observe the maximum removal percentage for this scenario was 76.33 % for a metal concentration of 10.44 $mg.L^{-1}$ with a system pH of 6.22 and an algae concentration of 1.14 $g.L^{-1}$.

The optimization was validated by five experimental replicates under the optimum condition obtained. It was observed that the experimental values obtained were in good agreement with the values predicted by the model, corroborating the ability of the model to predict the removal efficiency under the experimental conditions used. The corresponding experimental values was determined to be 83.82% ± 1.19 (p=0.320) for the first optimization (83.14%) and 76.54% ± 2.57 (p=0.861) for the second (76.33%). In both cases, p value was

greater than 0.05, which means that the null hypothesis (H_0: μ=83.14% and H_0: μ=76.33% for the first and second case, respectively) failed to be rejected.

5.5.2 Methylene blue biosorption

The values for the MB removal percentage obtained experimentally and those obtained by the model are shown in Table 13.

Table 13 - Actual and predicted values for the methylene blue percentage removal.

Run Order	Actual[a] (%)	Predict (%)	Residual
1	92.59±0.59	94.41	-1.82
2	95.45±0.51	97.14	-1.69
3	93.84±0.37	93.26	0.57
4	4.33±1.35	5.84	-1.51
5	93.52±0.70	91.7	1.82
6	95.54±0.28	92.03	3.51
7	3.71±0.44	2.02	1.69
8	1.14±0.77	4.65	-3.51
9	8.19±1.16	4.86	3.33
10	93.53±0.36	93.26	0.26
11	92.42±0.50	93.26	-0.84
12	93.92±1.35	97.25	-3.33
13	73.93±2.17	78.95	-5.02
14	91.71±0.79	86.69	5.02
15	92.01±0.81	90.5	1.51

[a]Mean ± standard deviation (N=3)

The models Linear, Interaction between two factors (2FI), Quadratic and Cubic models were evaluated for their adequacy by the sum of squares and model summary statistics, and the results are given in Table 14. For this study, the cubic model was considered aliased, not fitting precisely to the experimental design adopted and being necessary to augment the design if there was a desire to evaluate higher-order models. Among the models presented, the 2FI was considered as non-significant (p>0.05) in the process involving MB biosorption onto *C. pyrenoidosa*. Moreover, the model presented a low adjusted R^2, as well as the Linear model, which demonstrates that both, Linear and 2FI, did not present a good relationship between the independent variables and the response.

Table 14 - Adequacy of the models tested in terms of the sequential model sum of square and summary statistics for methylene blue biosorption process.

Source	Sum of squares	df[a]	Mean square	F value	p value
Sequential sum of squares					
Linear	6533.78	9	725.98	1302.35	0.0008
2FI	6419.67	6	1069.94	1919.41	0.0005
Quadratic[c]	114.22	3	38.07	68.3	0.0145
Cubic[d]	114.22	3	38.07	68.30	0.0145
Source	Std. Dev.	Predicted R^2	Adjusted R^2	R^2	PRESS[c]
Model Summary Statistics					
Linear	24.37	0.7129	0.6346	0.4662	12149.4975
2FI	28.33	0.7179	0.5063	-0.1614	26434.4028
Quadratic[c]	4.8	0.9949	0.9858	0.9196	1830.0136
Cubic[d]	0.7466	1.000	0.9997	[e]	[e]

[a]Degrees of freedom; [b]Standard deviation; [c]Model suggested; [d]Model aliased; [e]Statistic not defined

In contrast, the quadratic model presented greater significance ($p<0.001$), in addition to a high value of adjusted and predicted R^2, these two in concordance with each other (difference < 2). Concerning the MB biosorption process by *C. pyrenoidosa*, the model is able to explain 98.58% of the variations involved in the MB removal efficiency and does not explain only 1.52% of these variances. Moreover, the quadratic model had lower standard deviation compared to the others, and for these reasons were chosen to describe the biosorption process and subsequent analyzes.

$$\%Removal = 93.26 - 1.26D + 44.94B + 2.61C - 1.36DB + 5.12DC + 0.705BC - 2.25D^2 - 41.31B^2 - 3.07C^2 \quad (27)$$

In which D corresponds to MB concentration ($mg.L^{-1}$), B to pH and C to biosorbent concentration ($g.L^{-1}$).

The quadratic equation is presented in its coded form in Equation 27. The adequate precision was higher than the desired value (>4), indicating a good adequacy of the response obtained in relation to the associated noise. The model also presented a low coefficient of variation as a result of low deviations between the experimental and predicted values, demonstrating a high degree of precision and reliability in the experiments performed.

The quadratic model significance can be observed once again in the analysis of variance (ANOVA) presented in Table 15. The high values obtained for F-value corroborate the fact that most variations of the response factor can be explained by the models (TRIPATHI; SRIVASTAVA; KUMAR, 2009), which is in accordance to the results observed for the

correlation coefficient. The factors B, and B^2 were significants term. Thus, the removal efficiency presents a relationship both linear and quadratic with pH. This relation can be observed also by the pareto graph (Figure 16(a)).

Table 15 - Analysis of variance (ANOVA) results for response parameters.

Source	SS	df	Mean Square	F value	p value Prob. > F
Model	22646.3	9	2516.26	109.1	< 0.0001
D	12.6	1	12.6	0.546	0.4931
B	16159.5	1	16159.53	700.6	< 0.0001
C	54.65	1	54.65	2.37	0.1844
DB	7.37	1	7.37	0.32	0.5963
DC	104.76	1	104.76	4.54	0.0863
BC	1.99	1	1.99	0.086	0.7809
D^2	18.72	1	18.72	0.812	0.409
B^2	6302.25	1	6302.25	273.2	< 0.0001
C^2	34.89	1	34.89	1.51	0.2734
Residual	115.33	5	23.07		
Lack of Fit	114.22	3	38.07	68.3	0.0145
Pure Error	1.11	2	0.5574		
Std. Dev.	4.8		Adjusted R^2	0.9858	
Mean	68.39		Predicted R^2	0.9196	
C.V. %	7.02		Adeq. Precision	24.2846	
R^2	0.9949				

D: MB concentration ($mg.L^{-1}$); B: pH; C: biosorbent concentration ($g.L^{-1}$)

The data were also checked in terms of residuals normality when evaluating the normal probability plot, standardized by their estimated standard deviation. It is observed in Figure 16(c), that the points are distributed near the straight line, in addition to 95% of these contained in the range of (-6, +6), demonstrating that the normality assumption of the residuals is valid and without the presence of outliers. By observing the values predicted by the model and the actual values (obtained experimentally) in Figure 16(b), it can be seen that they satisfactorily distribute along the straight line, indicating that both the residuals related to the predicted values and the standard deviation associated to these parameters were low, characterizing a satisfactory adjustment.

Figure 16 - (a) Pareto chart of the standardized effects. (b) A residual plot showing the deviation of predicted values from experimental values for each case number. (c) Normal plot of residuals. (d) Plot of the experimental and predicted responses.

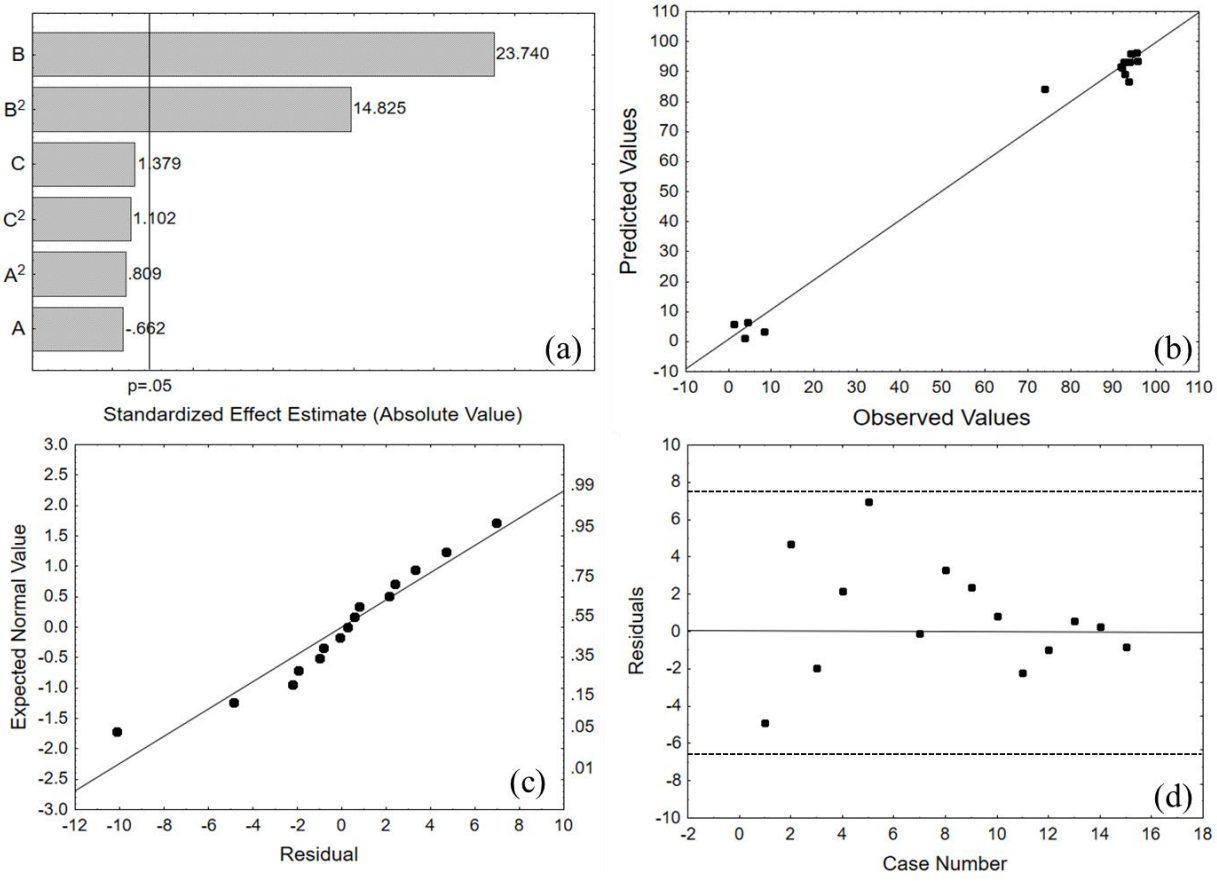

The residue analysis was complemented by evaluating the relation of the predicted values for the dependent variable throughout the experiments. In general, it is desired a random distribution of the points in order to characterize a constant variance of the errors. This behavior is seen in Figure 16(d), where a pattern is not observed. For these reasons, the random errors associated with the models can be considered random and distributed in a normal way, besides presenting a constant variance.

5.5.2.1 Effect of various parameters on MB removal efficiency

The effect of the chosen factors, and the relation between them, was evaluated through response surfaces as a function of two factors, keeping the third in its central value. Under these considerations, the MB removal efficiency varied between 1.14 - 95.54% for the biosorption by *C. pyrenoidosa*, as shown in Table 13. For a constant value of algae concentration (0.5 $g.L^{-1}$), Figure 17(a), *C. pyrenoidosa* showed an increase in the removal efficiency while increasing the pH, but no significant change was observed when the MB concentration was varied.

Figure 17 - 3D Response surface for %Removal versus pH and methylene blue concentration (a); versus methylene blue and biosorbent concentration and versus pH and biosorbent concentration.

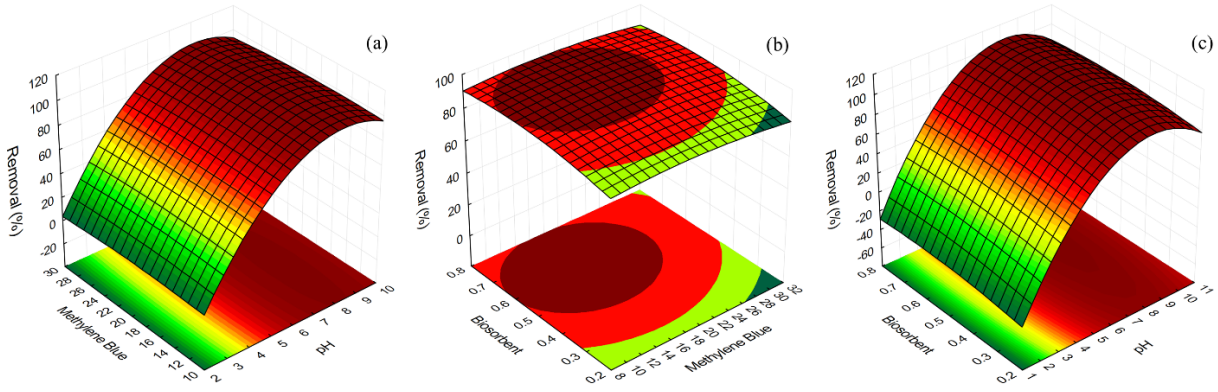

When the pH remained constant at 6, the removal efficiency slightly reduced for *C. pyrenoidosa* with an increase of MB concentration and reduction in the adsorbent concentration (Figure 17(b)). A reduction on percentage removal is also observed when the concentration of the biosorbent increased and the concentration of MB reduced. The fact of working with a low ratio between dye and adsorbent concentrations implies in a less availability of the surface area and active sites in which the adsorbate can interact, being these factors determinants in the biosorption process intensity. Kousha et al. (2012) also observed the reduction in adsorption capacity while evaluating the adsorption process of Acid Black 1 by *N. zanardini*, *S. glaucescens* and *S. marginatum* under conditions of high concentration of dye and low concentrations of adsorbent.

Finally, by keeping MB concentration constant at its central point (20 $mg.L^{-1}$) and evaluating the effect of the other two factors, it is again observed that pH significantly affects the *C. pyrenoidosa* MB uptake capacity (Figure 17(c)), but no significant effect was observed on the dependent variable when the adsorbent concentration was varied. The pH, as well as the surface area, is one of the factors that directly affects the biosorption intensity, since it determines the chemical species degree of distribution, besides the adsorbent surface charge (NASCIMENTO et al., 2014). In order to favor the biosorption process, it is necessary that the adsorbent and adsorbate present opposite charges, guaranteeing a greater electrostatic interaction between both. When evaluating the response surfaces, an expressive increase in the removal efficiency was observed when the pH was higher than 6. Above this value, the medium was sufficiently alkaline for the functional groups that constitute the active sites to release a proton to the solution. As the adsorbent is negatively charged, it favors the biosorption of the dye, which has a cationic character. Furthermore, at this pH the methylene blue is fully

presented in its cationic form (MB^+) (Figure 18), whereas in pH < 6 there may be other coexisting species such as MB^0 (KAZAK et al., 2017).

Figure 18 - Methylene blue species distribution over different pH.

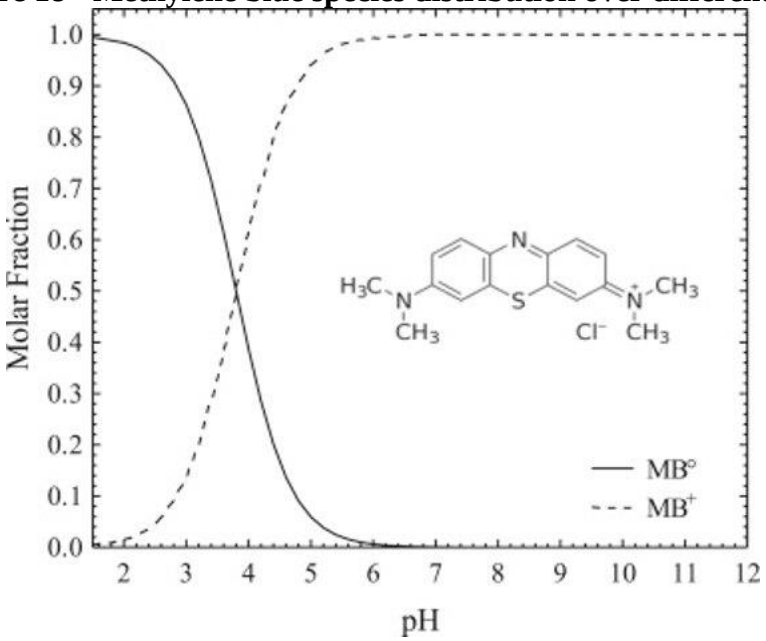

Source: SALAZAR-RABAGO et al., 2017

The observed behaviors corroborate the results obtained in the biosorbent characterization, which presented pH_{PZC} of 5.95. The expressive effect of pH on the removal efficiency was also observed in the study developed by Vijayaraghavan et al. (2015). The authors evaluated the uptake capacity of MB by the algae *Kappaphycus alverezzi*, observing an increase in the percentage of dye biosorption from 46% to 92% when the pH was varied from 5 to 8, respectively.

5.5.2.2 Process optimization

Process optimization was performed by combining the factor levels that simultaneously satisfy the requirements placed on each of the responses and factors. Based on that, two scenarios were considered aiming the maximization of MB removal, keeping the same importance (3) for all parameters. The first one maintained the factors within the study range evaluated, achieving a maximum removal efficiency of 98.203%, as given in Table 16. The second scenario considered a lower amount of adsorbent for a higher amount of adsorbate. For this case, an optimal value of 94,872% was obtained.

Table 16 - Optimization parameters and results obtained for the methylene blue biosorption process by *C. pyrenoidosa*.

			First case		Second case	
	Lower limit	Upper limit	Goal	Result	Goal	Result
D: Methylene blue ($mg.L^{-1}$)	10	30	in range	10.667	maximize	29.999
B: pH	2	10	in range	6.622	in range	8.293
C: Biosorbent ($g.L^{-1}$)	0.25	0.75	in range	0.288	minimize	0.252
Removal (%)	1.14	100	maximize	98.203	maximize	90.089

The optimization was validated by five experimental replicates under the optimum condition obtained. It was observed that the experimental values obtained were in good agreement with the values predicted by the model, corroborating the ability of the model to predict the removal efficiency under the experimental conditions used. The corresponding experimental values was determined to be 98.012% ± 1.22 (p=0.480) for the first optimization (98.203%) and 90.221% ± 1.79 (p=0.548) for the second (90.089%). In both cases, p value was greater than 0.05, which means that the null hypothesis (H_0: μ=98.203% and H_0: μ=90.089% for the first and second case, respectively) failed to be rejected.

5.6 Regeneration Study

For large-scale application, regeneration and reusability are the vital biosorbent characteristics, since the ability to reuse a biosorbent is a crucial parameter for the decontamination process from the economic point of view. For the regeneration study, the biosorbent was loaded using optimized conditions for both copper and MB removal and the results are presented in Figure 19 and Figure 20, respectively.

Figure 19 - Removal (%) and *C. pyrenoidosa* regeneration efficiency (%) for successive cycles regarding copper biosorption process.

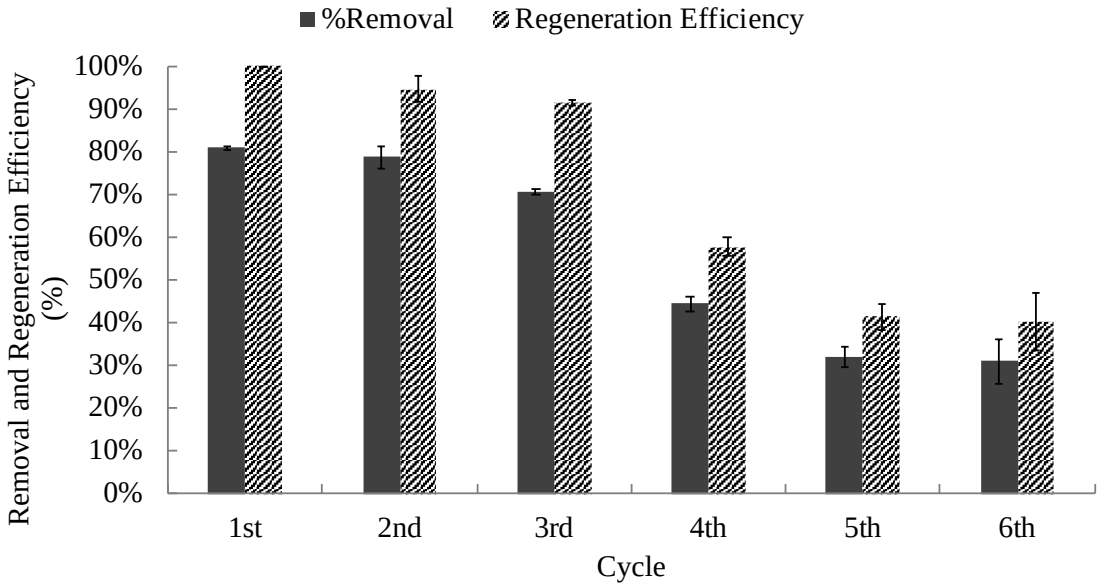

Figure 20 - Removal (%) and *C. pyrenoidosa* regeneration efficiency (%) for successive cycles regarding methylene blue biosorption process.

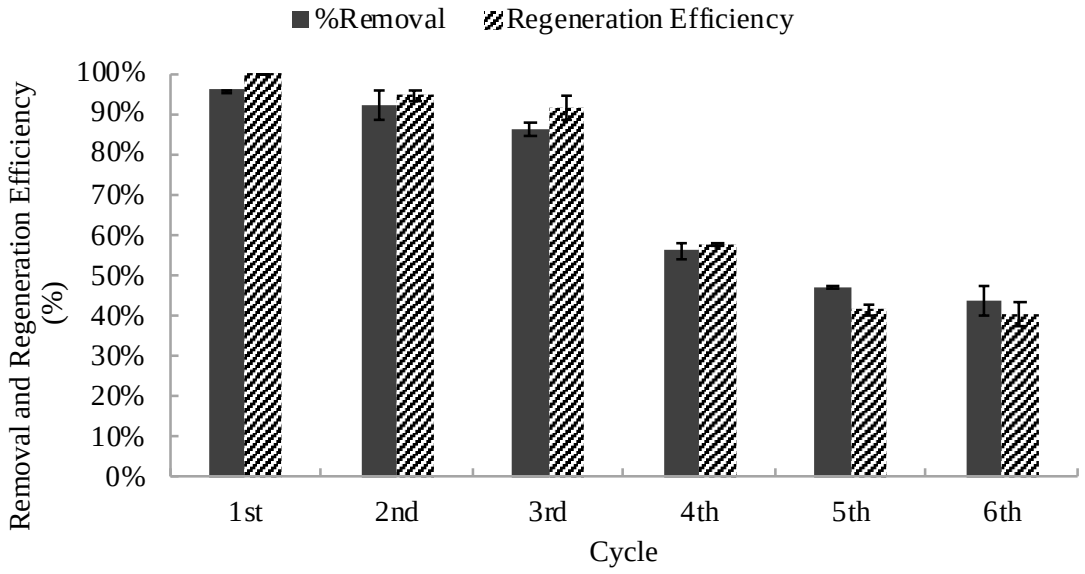

Until the third cycle, a removal reduction of only 12.86% was observed when the copper biosorption process was considered. From this cycle the forward the removal fell more significantly, a consequence of the reduction of the efficiency of regeneration, reaching a decay of 61.80% in the sixth cycle. The biosorbent regeneration for the process involving the MB biosorption presented similar behavior. Up to the third cycle, there was a reduction of only 10.35% in the removal percentage, and 54.36% when compared to the sixth cycle. The values

obtained are slightly better when compared to those obtained for the biosorbent regeneration when considering a copper biosorption process.

The low cost of production of microalgae and their high availability compensates for the fact that this adsorbent adequately supports until the third cycle (MUÑOZ et al., 2006). Similarly, Asfaram et al. (2018), which tested the reusability of nanoparticles supported on dead cells of *Yarrowia lipolytica* as a novel biosorbent for the removal of azo food dyes, found a more significant reduction in the removal of food dyes from the 3rd cycle of adsorption.

5.7 Ion exchange mechanism

The characteristics associated with the biosorbent and adsorbate determine the mechanism involved in the biosorption process, which include electrostatic interactions, surface precipitation, chemical reactions, ion exchange, or a combination of them. However, the ions exchange has predominated in several biosorption cases (MITROGIANNIS et al., 2015; CHOJNACKA; CHOJNACKI; GÓRECKA, 2005; CHEN et al., 2017). The Ca, Mg and Na metals observed in the EDS analysis were quantified after the biosorption process at concentrations ranging from 0.665-2.232 $mg.L^{-1}$, while the copper concentration was reduced by approximately 85% (Table 17).

Table 17 - Amount of cations released from *C. pyrenoidosa* after copper and methylene blue biosorption.

	Total adsorbate bound ($mg.L^{-1}$)	Total H^+ bound ($mg.L^{-1}$)	Ca^{2+} ($mg.L^{-1}$)	Mg^{2+} ($mg.L^{-1}$)	Na^+ ($mg.L^{-1}$)	$R_{b/r}$
Blank	0.000	2.951E-4 ± 9.118E-5	0.000	0.000	0.257 ± 0.024	0.995 ± 0.090
C. pyrenoidosa with Cu^{2+}	4.126 ± 0.019	2.4206E-3 ± 1.707E-4	0.665 ± 0.059	2.292 ± 0.123	1.025 ± 0.077	
C. pyrenoidosa with MB	4.799 ± 0.047	2.420E-03 ± 1.010E-4	0.957 ± 0.087	3.225 ± 0.091	1.337 ± 0.148	0.9891 ± 0.084

Based on the total amount of cations released to the medium, associated with a $R_{b/r}$ value close to 1 (CHOJNACKA; CHOJNACKI; GÓRECKA, 2005), it is suggested a predominance of the ion exchange mechanism in either copper or MB biosorption. This mechanism between the copper ions and the exchangeable cations from the biomass surface can be described from Equations 28 to 30, where S represents the surface of *C. pyrenoidosa*. For MB biosorption, the mechanism is described in Equations 31 to 33.

$$S - Na + Cu^{2+} \rightarrow S - Cu + 2Na^{+} \quad (28)$$

$$S - Ca + Cu^{2+} \rightarrow S - Cu + Ca^{2+} \quad (29)$$

$$S - Mg + Cu^{2+} \rightarrow S - Cu + Mg^{2+} \quad (30)$$

$$S - Na + MB^{+} \rightarrow S - MB + Na^{+} \quad (31)$$

$$S - Ca + 2MB^{+} \rightarrow S - MB + Ca^{2+} \quad (32)$$

$$S - Mg + 2MB^{+} \rightarrow S - MB + Mg^{2+} \quad (33)$$

6. FINAL CONSIDERATIONS

The biomass presented significant interactions for both copper and MB biosorption. The change in transmittance observed by infrared spectra for all functional groups, and specifically in 1643 cm^{-1}, associated with a low value of enthalpy change, suggested a physical biosorption, predominating an ion exchange mechanism. Different functional groups representing mainly proteins and polysaccharides was also identified by FTIR spectra. The thermogravimetric analysis affirmed these results, characterizing a microalgae consisting mainly of proteins and carbohydrates.

The equilibrium was best described by Langmuir's isotherm in both cases, characterizing the process by the formation of a monolayer. Other models presented a satisfactory fit to the data once they present high R^2 values and low values of R^2, SSE, $CFEF$ and χ^2. In both copper and MB biosorption, the Dubinin-Radushkevich isotherm indicated values of $E < 8.0$ ($kJ.mol^{-1}$), once again confirming the thermodynamic and FTIR results. The kinetic equilibrium was observed after 30 minutes of the beginning of the process and was best described by a pseudo second order model.

The process regarding the biosorption of copper was characterized as endothermic, while the biosorption of MB was exothermic. In any case, a thermodynamically spontaneous nature for the biosorption process was observed for the temperature range evaluated. Regarding reusability and removal efficiency, the biosorbent was stable until the third regeneration cycle, noticing a reduction of only 12.86% in relation to the first cycle when the copper biosorption process was considered while 10.35% reduction was observed when the MB biosorption was evaluated.

The quadratic equation for copper and MB removal by *C. pyrenoidosa* obtained through Box-Behnken design presented low residues and a high degree of reliability for predictive purposes. Moreover, the response surface proved to be an efficient tool for optimization, converting the biosorption process to a mathematical model which was used to locate the optimal point of the process. For the optimization a maximum removal efficiency was found to be 83.14% for copper ions and 98.20% for methylene blue ions.

7. SUGGESTIONS FOR FUTURE WORKS

i. Another way of conducting the adsorption experiments, different than the batch mode adopted in this study, could be evaluated and compared. One of them is the “fix bed” adsorption mode.

ii. The use of functionalized biosorbents implies higher costs in obtaining the final biosorbent. However, depending on the results obtained, this could be overcome by a possible significant increase in the material biosorption capacity. Therefore, acid or basic treated microalgae could be tested, and the results compared.

iii. A common way to express the results is through the material adsorption capacity (q_e), which could be a possible response to be optimized by the aid of response surface methodology.

iv. In general, wastewaters/surface waters contain various types of suspended and dissolved compounds apart from the dyes and heavy metals. The presence of ions leads to high ionic strength, which may significantly affect the performance of the biosorption process. An evaluation of the ionic strength involved in biosorption of copper and MB could be performed in order to better understand the process.

v. There is a lack on biosorption studies that consider the synergetic effect of inorganic and organic compounds in a multicomponent system. Further analysis could be made in order to consider it.

vi. Other biomass, mainly lignocellulosic, with easy access, could be tested for the biosorption of methylene blue and copper ions.

REFERENCES

AHARONI, C.; UNGARISH, M. Kinetics of activated chemisorption. Part 2. - Theoretical models. **Journal of the Chemical Society, Faraday Transactions 1: Physical Chemistry in Condensed Phases**, v. 73, p. 456–464, 1977.

AKSU, Z.; DÖNMEZ, G. Binary biosorption of cadmium (II) and nickel (II) onto dried *Chlorella vulgaris*: Co-ion effect on mono-component isotherm parameters. **Process Biochemistry**, v. 41, n. 4, p. 860-868, 2006.

ARAÚJO, C. S. T. et al. Elucidation of mechanism involved in adsorption of Pb(II) onto lobeira fruit (*Solanum lycocarpum*) using Langmuir, Freundlich and Temkin isotherms. **Microchemical Journal**, v. 137, p. 348–354, 1 mar. 2018.

ASFARAM, A. et al. Preparation and Characterization of $Mn_{0.4}Zn_{0.6}Fe_2O_4$ Nanoparticles Supported on Dead Cells of Yarrowia lipolytica as a Novel and Efficient Adsorbent/Biosorbent Composite for the Removal of Azo Food Dyes: Central Composite Design Optimization Study. **ACS Sustainable Chemistry & Engineering**, v. 6, n. 4, p. 4549–4563, 2 abr. 2018.

BACH, Q.-V.; CHEN, W.-H. Pyrolysis characteristics and kinetics of microalgae via thermogravimetric analysis (TGA): A state-of-the-art review. **Bioresource Technology**, v. 246, p. 88–100, 1 dez. 2017.

BALTAZAR, M. DOS P. G. et al. Copper biosorption by *Rhodococcus erythropolis* isolated from the Sossego Mine – PA – Brazil. **Journal of Materials Research and Technology**, jun. 2018.

BLINOVÁ, L.; BARTOŠOVÁ, A.; GERULOVÁ, K. Cultivation of microalgae (*Chlorella vulgaris*) for biodiesel production. **Research Papers Faculty of Materials Science and Technology Slovak University of Technology**, v. 23, n. 36, p. 87-95, 2015.

BOLLER, M. Tracking heavy metals reveals sustainability deficits of urban drainage systems. **Water Science and Technology**, v. 35, n. 9, 1997.

BONILLA-PETRICIOLET, A.; MENDOZA CASTILLO, D. I.; REYNEL-ÁVILA, H. E. **Adsorption Processes for Water Treatment and Purification**. 2017.

BROWN, R. A.; BOX, G. E. P.; DRAPER, N. R. Empirical Model-Building and Response Surfaces. **Biometrics**, v. 46, n. 1, p. 283, 1990.

CALADO, V.; MONTGOMERY, D. **Planejamento de experimentos usando o Statistica**.

2003.

CARDOSO, N. F. et al. Comparison of *Spirulina platensis* microalgae and commercial activated carbon as adsorbents for the removal of Reactive Red 120 dye from aqueous effluents. **Journal of Hazardous Materials**, v. 241–242, p. 146–153, 30 nov. 2012.

CAZETTA, M. L. et al. Optimization study for sorbitol production by *Zymomonas mobilis* in sugar cane molasses. **Process Biochemistry**, 2005.

CHARERNTANYARAK, L. Heavy metals removal by chemical coagulation and precipitation. **Water Science and Technology**, v. 39, n. 10–11, 1999.

CHEN, L. et al. High performance agar/graphene oxide composite aerogel for methylene blue removal. **Carbohydrate Polymers**, v. 155, p. 345–353, jan. 2017.

CHEN, S. et al. Adsorption of hexavalent chromium from aqueous solution by modified corn stalk: A fixed-bed column study. **Bioresource Technology**, v. 113, p. 114–120, jun. 2012.

CHEN, T. et al. Adsorption of cadmium by biochar derived from municipal sewage sludge: impact factors and adsorption mechanism. **Chemosphere**, v. 134, p. 286-293, 2015.

CHEUNG, W. H.; SZETO, Y. S.; MCKAY, G. Intraparticle diffusion processes during acid dye adsorption onto chitosan. **Bioresource Technology**, v. 98, n. 15, p. 2897–2904, nov. 2007.

CHOJNACKA, K.; CHOJNACKI, A.; GÓRECKA, H. Biosorption of Cr^{3+}, Cd^{2+} and Cu^{2+} ions by blue–green algae *Spirulina sp.*: kinetics, equilibrium and the mechanism of the process. **Chemosphere**, v. 59, n. 1, p. 75–84, mar. 2005.

COUTO, C. F.; MORAVIA, W. G.; AMARAL, M. C. S. Integration of microfiltration and nanofiltration to promote textile effluent reuse. **Clean Technologies and Environmental Policy**, 2017.

DĄBROWSKI, A. et al. Selective removal of the heavy metal ions from waters and industrial wastewaters by ion-exchange method. **Chemosphere**, v. 56, n. 2, p. 91–106, jul. 2004.

DAHIYA, A. **In Bioenergy: Biomass to Biofuel.** v. 1, p. 219-238, 2014.

DEMIRBAS, A. Heavy metal adsorption onto agro-based waste materials: A review. **Journal of Hazardous Materials**, v. 157, n. 2–3, p. 220–229, set. 2008.

DHIR, B. Potential of biological materials for removing heavy metals from wastewater. **Environmental Science and Pollution Research**, v. 21, n. 3, p. 1614–1627, 2 fev. 2014.

DINU, M. V.; DRAGAN, E. S. Evaluation of Cu^{2+}, Co^{2+} and Ni^{2+} ions removal from aqueous

solution using a novel chitosan/clinoptilolite composite: Kinetics and isotherms. **Chemical Engineering Journal**, v. 160, n. 1, p. 157–163. 2010.

DOTTO, G. L.; CADAVAL, T. R. S.; PINTO, L. A. A. Use of *Spirulina platensis* micro and nanoparticles for the removal synthetic dyes from aqueous solutions by biosorption. **Process Biochemistry**, v. 47, n. 9, p. 1335-1343, 2012.

DUBININ, M. M. The Potential Theory of Adsorption of Gases and Vapors for Adsorbents with Energetically Nonuniform Surfaces. **Chemical Reviews**, v. 60, n. 2, p. 235–241, 1 abr. 1960.

DUMAS, P.; MILLER, L. **The use of synchrotron infrared microspectroscopy in biological and biomedical investigations**. Vibrational Spectroscopy. **Anais**. 2003.

EPA, U. S. E. P. A. **Copper in Drinking Water: Health Effects and How to Reduce Exposure Fact Sheet - EH: Minnesota Department of Health**. 2005. Disponível em: <http://www.health.state.mn.us/divs/eh/water/factsheet/com/copper.html>.

FAN, S. et al. Removal of methylene blue from aqueous solution by sewage sludge-derived biochar: Adsorption kinetics, equilibrium, thermodynamics and mechanism. **Journal of Environmental Chemical Engineering**, v. 5, n. 1, p. 601–611, 1 fev. 2017.

FEBRIANTO, J. et al. Equilibrium and kinetic studies in adsorption of heavy metals using biosorbent: A summary of recent studies. **Journal of Hazardous Materials**, v. 162, n. 2–3, p. 616–645, 2009.

FOO, K. Y.; HAMEED, B. H. Insights into the modeling of adsorption isotherm systems. **Chemical Engineering Journal**, v. 156, n. 1, p. 2–10, 1 jan. 2010.

FOROUGHI-DAHR, M. et al. Adsorption Characteristics of Congo Red from Aqueous Solution onto Tea Waste. **Chemical Engineering Communications**, v. 202, n. 2, p. 181–193, 15 fev. 2015a.

FOROUGHI-DAHR, M. et al. Experimental study on the adsorptive behavior of Congo red in cationic surfactant-modified tea waste. **Process Safety and Environmental Protection**, v. 95, p. 226–236, maio 2015b.

FREITAS, F. B. A. DE; CÂMARA, M. Y. DE F.; FREIRE, M. D. F. **Determinação do PCZ de adsorventes naturais utilizados na remoção de contaminantes em soluções aquosas**. Anais do 5º Encontro Regional de Química & 4º Encontro Nacional de Química. **Anais**. São Paulo: Editora Edgard Blücher, nov. 2015. Disponível em:

<http://www.proceedings.blucher.com.br/article-details/22117>. Acesso em: 30 jul. 2018.

FREUNDLICH, H. M. F. Over the Adsorption in Solution. **The Journal of Physical Chemistry**, 1906.

FU, J. et al. Adsorption of methylene blue by a high-efficiency adsorbent (polydopamine microspheres): Kinetics, isotherm, thermodynamics and mechanism analysis. **Chemical Engineering Journal**, v. 259, p. 53–61, 1 jan. 2015.

GAUTAM, R. K. et al. Biomass-derived biosorbents for metal ions sequestration: Adsorbent modification and activation methods and adsorbent regeneration. **Journal of Environmental Chemical Engineering**, v. 2, n. 1, p. 239–259, mar. 2014.

GEORGIN, J. et al. Biosorption of cationic dyes by Pará chestnut husk (*Bertholletia excelsa*). **Water Science and Technology**, 2018.

GIUNTA, A.; WATSON, L. A comparison of approximation modeling techniques - Polynomial versus interpolating models. **7th AIAA/USAF/NASA/ISSMO Symposium on Multidisciplinary Analysis and Optimization**, 1998.

GÓMEZ, D. N. **Potencial da casca de camarão para remediação de águas contaminadas com drenagem ácida mineral visando seu reuso secundário não potável**. 2014.

GUPTA, V. K.; SALEH, T. A. Sorption of pollutants by porous carbon, carbon nanotubes and fullerene- An overview. **Environmental Science and Pollution Research**, v. 20, n. 5, p. 2828–2843, 21 maio 2013.

HAN, R. et al. Characterization of modified wheat straw, kinetic and equilibrium study about copper ion and methylene blue adsorption in batch mode. **Carbohydrate Polymers**, v. 79, n. 4, p. 1140–1149, 17 mar. 2010.

HARRINGTON, E. C. The desirability function. **Industrial quality control**, v. 21, n. 10, p. 494–498, 1965.

HASSAN, A. F.; ELHADIDY, H. Production of activated carbons from waste carpets and its application in methylene blue adsorption: Kinetic and thermodynamic studies. **Journal of Environmental Chemical Engineering**, v. 5, n. 1, p. 955–963, 1 fev. 2017.

HO, Y. S.; PORTER, J. F.; MCKAY, G. Equilibrium Isotherm Studies for the Sorption of Divalent Metal Ions onto Peat: Copper, Nickel and Lead Single Component Systems. **Water, Air, and Soil Pollution**, v. 141, n. 1, p. 1–33, nov. 2002.

HOU, H. et al. Removal of Congo red dye from aqueous solution with hydroxyapatite/chitosan composite. **Chemical Engineering Journal**, v. 211–212, p. 336–342, nov. 2012.

JAIN, C. K.; MALIK, D. S.; YADAV, A. K. Applicability of plant based biosorbents in the removal of heavy metals: a review. **Environmental Processes**, v. 3, n. 2, p. 495–523, 28 jun. 2016.

KAZAK, O. et al. A novel red mud@sucrose based carbon composite: Preparation, characterization and its adsorption performance toward methylene blue in aqueous solution. **Journal of Environmental Chemical Engineering**, v. 5, n. 3, p. 2639–2647, 1 jun. 2017.

KAZEMI, P. et al. Pertraction of methylene blue using a mixture of D_2EHPA/M_2EHPA and sesame oil as a liquid membrane. **Chemical Papers**, v. 67, n. 7, p. 722–729, jul. 2013.

KHATAEE, A. R.; VAFAEI, F.; JANNATKHAH, M. Biosorption of three textile dyes from contaminated water by filamentous green algal *Spirogyra sp.*: Kinetic, isotherm and thermodynamic studies. **International Biodeterioration and Biodegradation**, 2013.

KIM, Y. et al. Arsenic Removal Using Mesoporous Alumina Prepared via a Templating Method. **Environmental Science and Technology**, v. 38, n. 3, p. 924–931, 2004.

KOUSHA, M. et al. Box–Behnken design optimization of Acid Black 1 dye biosorption by different brown macroalgae. **Chemical Engineering Journal**, v. 179, p. 158–168, 1 jan. 2012.

LAGERGREN, S. **Zur Theorie der sogenannten Adsorption geloster Stoffe**. 1898.

LAMBROPOULOU, D. et al. Degradation of venlafaxine using TiO_2/UV process: Kinetic studies, RSM optimization, identification of transformation products and toxicity evaluation. **Journal of Hazardous Materials**, 2017.

LANGMUIR, I. The adsorption of gases on plane surfaces of glass, mica and platinum. **Journal of the American Chemical Society**, 1918.

LARGITTE, L.; PASQUIER, R. A review of the kinetics adsorption models and their application to the adsorption of lead by an activated carbon. **Chemical Engineering Research and Design**, v. 109, p. 495–504, 2016.

LEE, L. Y. et al. Effective removal of Acid Blue 113 dye using overripe *Cucumis sativus* peel as an eco-friendly biosorbent from agricultural residue. **Journal of Cleaner Production**, v. 113, p. 194–203, 1 fev. 2016.

LEE, S.-M.; LALDAWNGLIANA, C.; TIWARI, D. Iron oxide nano-particles-immobilized-

sand material in the treatment of Cu(II), Cd(II) and Pb(II) contaminated waste waters. **Chemical Engineering Journal**, v. 195–196, p. 103–111, jul. 2012.

LI, X. et al. Equilibrium and kinetic studies of copper biosorption by dead *Ceriporia lacerata* biomass isolated from the litter of an invasive plant in China. **Journal of Environmental Health Science and Engineering**, v. 13, n. 1, p. 37, 25 dez. 2015.

MANZOOR, Q. et al. Organic acids pretreatment effect on *Rosa bourbonia* phyto-biomass for removal of Pb(II) and Cu(II) from aqueous media. **Bioresource Technology**, 2013.

MARTÍN-LARA, M. A. et al. Binary biosorption of copper and lead onto pine cone shell in batch reactors and in fixed bed columns. **International Journal of Mineral Processing**, v. 148, p. 72–82, mar. 2016.

MIRABOUTALEBI, S. M. et al. Methylene blue adsorption via maize silk powder: Kinetic, equilibrium, thermodynamic studies and residual error analysis. **Process Safety and Environmental Protection**, 2017.

MITROGIANNIS, D. et al. Biosorption of methylene blue onto *Arthrospira platensis* biomass: Kinetic, equilibrium and thermodynamic studies. **Journal of Environmental Chemical Engineering**, 2015.

MORONEY, J. V.; YNALVEZ, R. A. Algal Photosynthesis. **eLS**. John Wiley & Sons Ltd, Chichester. 2009.

MOURA, M. C. P. DE A. **Utilização de microemulsões como agentes modificadores de superfícies para remoção de íons metálicos**. Universidade Federal do Rio Grande do Norte, 2001.

MOURABET, M. et al. Removal of fluoride from aqueous solution by adsorption on Apatitic tricalcium phosphate using Box-Behnken design and desirability function. **Applied Surface Science**, 2012.

MOURAD, K. et al. Modeling Tool for Air Stripping and Carbon Adsorbers to Remove Trace Organic Contaminants. **International Journal of Thermal and Environmental Engineering**, v. 4, n. 1, p. 99–106, 15 mar. 2012.

MUÑOZ, R. et al. Sequential removal of heavy metals ions and organic pollutants using an algal-bacterial consortium. **Chemosphere**, 2006.

NASCIMENTO, R. F. et al. **Adsorção: Aspectos teóricos e aplicações ambientais**. 2014.

NEBAGHE, K. C. et al. Comparison of linear and non-linear method for determination of optimum equilibrium isotherm for adsorption of copper(II) onto treated Martil sand. **Fluid Phase Equilibria**, 2016.

NGAH, W. S. W.; HANAFIAH, M. A. K. M. Biosorption of copper ions from dilute aqueous solutions on base treatedrubber (*Hevea brasiliensis*) leaves powder: kinetics, isotherm, and biosorption mechanisms. **Journal of Environmental Sciences**, v. 20, n. 10, p. 1168–1176, 1 jan. 2008.

O'MAHONY, T.; GUIBAL, E.; TOBIN, J. . Reactive dye biosorption by *Rhizopus arrhizus* biomass. **Enzyme and Microbial Technology**, v. 31, n. 4, p. 456–463, set. 2002.

OVEISI, F. et al. Effective removal of mercury from aqueous solution using thiol-functionalized magnetic nanoparticles. **Environmental Nanotechnology, Monitoring & Management**, 2017.

PATHANIA, D.; SHARMA, S.; SINGH, P. Removal of methylene blue by adsorption onto activated carbon developed from *Ficus carica* bast. **Arabian Journal of Chemistry**, 2017.

PERES, E. C. et al. Treatment of leachates containing cobalt by adsorption on *Spirulina sp*. and activated charcoal. **Journal of Environmental Chemical Engineering**, 2018.

PETER ATKINS, J. DE P. **Atkins' Physical Chemistry**. 2006.

PEYDAYESH, M.; RAHBAR-KELISHAMI, A. Adsorption of methylene blue onto *Platanus orientalis* leaf powder: Kinetic, equilibrium and thermodynamic studies. **Journal of Industrial and Engineering Chemistry**, 2015.

PHUKAN, M. M. et al. Microalgae *Chlorella* as a potential bio-energy feedstock. **Applied Energy**, 2011.

PINO, G. A. H. **Biossorção De Metais Pesados Utilizando Pó Da Casca De Coco Verde (*Cocos Nucifera*)**. Rio de Janeiro, Brazil: Pontifícia Universidade Católica do Rio de Janeiro, 30 mar. 2005.

PIRES, J. C. M. **Handbook of Marine Microalgae**. 2015.

PRAKASH MARAN, J. et al. Box-Behnken design based statistical modeling for ultrasound-assisted extraction of corn silk polysaccharide. **Carbohydrate Polymers**, 2013.

QDAIS, H. A.; MOUSSA, H. Removal of heavy metals from wastewater by membrane processes: a comparative study. **Desalination**, v. 164, p. 105–110, 2004.

QIU, H. et al. Critical review in adsorption kinetic models. **Journal of Zhejiang University-SCIENCE A**, v. 10, n. 5, p. 716–724, 2009.

RASHID, N. et al. Current status, issues and developments in microalgae derived biodiesel production. **Renewable and Sustainable Energy Reviews**, v. 40, p.760–778, 2014.

RAULINO, G. S. C. **Biossorção em sistema multielementar dos íons Pb(II), Cu(II), Ni(II), Cd(II) e Zn(II) em solução aquosa usando a vagem seca do feijão (*Phaseolus vulgaris L.*) modificada: otimização usando planejamento fatorial**. 2016.

REGTI, A. et al. Use of response factorial design for process optimization of basic dye adsorption onto activated carbon derived from *Persea* species. **Microchemical Journal**, 2017.

RIZZO, A. M. et al. Characterization of microalga *Chlorella* as a fuel and its thermogravimetric behavior. **Applied Energy**, 2013.

RODRIGUES FILHO, G. M. **ADSORÇÃO DO CORANTE AMARELO REATIVO BF-4G 200% por argila esmectita**. 2012.

ROMERO-CANO, L. A. et al. Functionalized adsorbents prepared from fruit peels: Equilibrium, kinetic and thermodynamic studies for copper adsorption in aqueous solution. **Journal of Cleaner Production**, 2017.

RONDA, A. et al. Copper biosorption in the presence of lead onto olive stone and pine bark in batch and continuous systems. **Environmental Progress & Sustainable Energy**, v. 33, n. 1, p. 192–204, abr. 2014.

SALAZAR-RABAGO, J. J. et al. Biosorption mechanism of Methylene Blue from aqueous solution onto White Pine (*Pinus durangensis*) sawdust: Effect of operating conditions. **Sustainable Environment Research**, v. 27, n. 1, p. 32–40, 1 jan. 2017.

SALEH, T. A.; SARI, A.; TUZEN, M. Optimization of parameters with experimental design for the adsorption of mercury using polyethylenimine modified-activated carbon. **Journal of Environmental Chemical Engineering**, 2017.

SALLEH, M. A. M. et al. Cationic and anionic dye adsorption by agricultural solid wastes: A comprehensive review. **Desalination**, v. 280, n. 1–3, p. 1–13, out. 2011.

SCHULTZ, D. R. **Recuperação de metais pesados (Pb, Cu e Ni) de efluentes or utilizando reator eletroquímico de leito particulado**. 2003.

SHI, C. et al. Porous chitosan/hydroxyapatite composite membrane for dyes static and dynamic

removal from aqueous solution. **Journal of Hazardous Materials**, v. 338, p. 241–249, set. 2017.

SILVA, M. C. M. DA. **Avaliação da adsorção de cobre a partir de carvão obtido quimicamente do bagaço de cana de açúcar**. Universidade Federal do Rio Grande do Norte, 9 jan. 2017. Disponível em: <https://monografias.ufrn.br/jspui/handle/123456789/5312>. Acesso em: 23 out. 2018.

SILVA, R. P. DA. **Remoção de metais pesados em efluentes sintéticos utilizando vermiculita como adsorvente**. 2010.

SOLISIO, C.; AL ARNI, S.; CONVERTI, A. Adsorption of inorganic mercury from aqueous solutions onto dry biomass of *Chlorella vulgaris* : kinetic and isotherm study. **Environmental Technology**, p. 1–9, 11 nov. 2017.

SOLTANI, R. D. C. et al. Photoelectrochemical treatment of ammonium using seawater as a natural supporting electrolyte. **Chemistry and Ecology**, 2013.

SOUZA, A. M. et al. Seasonal study of concentration of heavy metals in waters from lower São Francisco River basin, Brazil. **Brazilian Journal of Biology**, v. 76, n. 4, p. 967–974, maio 2016.

STUART, B. H. **Infrared Spectroscopy: Fundamentals and Applications**. 2004.

SUÁREZ, E. et al. Isolation, characterization and structural determination of a unique type of arabinogalactan from an immunostimulatory extract of *Chlorella pyrenoidosa*. **Carbohydrate research**, v. 340, n. 8, p. 1489-1498, 2005.

TAN, C. Y. et al. Biosorption of Basic Orange from aqueous solution onto dried *A. filiculoides* biomass: Equilibrium, kinetic and FTIR studies. **Desalination**, 2011.

TEMKIN, I., M. Kinetics of ammonia synthesis on promoted iron catalysts. **Acta Physiochim. URSS**, v. 12, p. 327–356, 1940.

TERBLANCHE, U. et al. Screening of Variables Influencing Extraction Yield of *Cotyledon orbiculata*: 2^3 Full Factorial Design. **International Journal of Pharmacognosy and Phytochemical Research**, v. 9, n. 3, p. 303–312, 2017.

TOROPOV, V. et al. Refinements in the multi-point approximation method to reduce the effects of noisy structural responses. **6th Symposium on Multidisciplinary Analysis and Optimization**, 1996.

TRIPATHI, P.; SRIVASTAVA, V. C.; KUMAR, A. Optimization of an azo dye batch adsorption parameters using Box–Behnken design. **Desalination**, v. 249, n. 3, p. 1273–1279, 25 dez. 2009.

UDDIN, M. T. et al. Adsorptive removal of methylene blue by tea waste. **Journal of Hazardous Materials**, 2009.

VAN CAMPEN, D.H., NAGTEGAAL, R. AND S.; A.J.G. **Approximation methods in structural optimization using experimental designs for multiple responses**. p. 205–228., 1990.

VAZ, M. G. et al. Methylene Blue Adsorption on Chitosan-g-Poly(Acrylic Acid)/Rice Husk Ash Superabsorbent Composite: Kinetics, Equilibrium, and Thermodynamics. **Water, Air, & Soil Pollution**, v. 228, n. 1, p. 14, 8 jan. 2017.

VIDAL, C. B. et al. Multielement adsorption of metal ions using Tururi fibers (*Manicaria Saccifera*): experiments, mathematical modeling and numerical simulation. **Desalination and Water Treatment**, 2016.

VIJAYARAGHAVAN, J. et al. Evaluation of Red Marine Alga *Kappaphycus alvarezii* as Biosorbent for Methylene Blue: Isotherm, Kinetic, and Mechanism Studies. **Separation Science and Technology**, v. 50, n. 8, p. 1120–1126, 24 maio 2015.

VILLANUEVA, R. O. C. Biosorption of heavy metals by use of microbial biomass. **Revista Latinoamericana de Microbiología**, v. 42, n. 3, p. 131-143, 2000.

WOLKERS, W. F. et al. A Fourier-transform infrared spectroscopy study of sugar glasses. **Carbohydrate Research**, 2004.

WONG, C. et al. Biosorption of copper by endophytic fungi isolated from *Nepenthes ampullaria*. **Letters in Applied Microbiology**, v. 67, n. 4, p. 384–391, out. 2018.

WU, Y. et al. Adsorption of Copper Ions and Methylene Blue in a Single and Binary System on Wheat Straw. **Journal of Chemical & Engineering Data**, v. 54, n. 12, p. 3229–3234, 10 dez. 2009.

XIA, S. et al. Photocatalytic degradation of methylene blue with a nanocomposite system: synthesis, photocatalysis and degradation pathways. **Phys. Chem. Chem. Phys.**, v. 17, n. 7, p. 5345–5351, 2015.

XU, J. et al. **A review of functionalized carbon nanotubes and graphene for heavy metal**

adsorption from water: Preparation, application, and mechanismChemosphere, 2018.

YAGUB, M. T. et al. Dye and its removal from aqueous solution by adsorption: A review. **Advances in Colloid and Interface Science**, v. 209, p. 172–184, 1 jul. 2014.

YAGUB, M. T.; SEN, T. K.; ANG, M. Removal of cationic dye methylene blue (MB) from aqueous solution by ground raw and base modified pine cone powder. **Environmental Earth Sciences**, v. 71, n. 4, p. 1507–1519, fev. 2014.

ZERAATKAR, A. K. et al. Potential use of algae for heavy metal bioremediation, a critical review. **Journal of Environmental Management**, v. 181, p. 817–831, out. 2016.

ZHANG, Y.-Z. et al. Removal of Copper Ions and Methylene Blue from Aqueous Solution Using Chemically Modified Mixed Hardwoods Powder as a Biosorbent. **Industrial & Engineering Chemistry Research**, v. 53, n. 11, p. 4247–4253, 19 mar. 2014.

ZOU, W. et al. Characterization of modified sawdust, kinetic and equilibrium study about methylene blue adsorption in batch mode. **Korean Journal of Chemical Engineering**, 2013.